

Journal of Materials Chemistry B

Accepted Manuscript

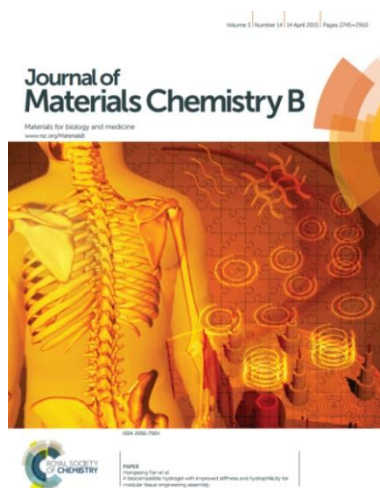


This is an *Accepted Manuscript*, which has been through the Royal Society of Chemistry peer review process and has been accepted for publication.

Accepted Manuscripts are published online shortly after acceptance, before technical editing, formatting and proof reading. Using this free service, authors can make their results available to the community, in citable form, before we publish the edited article. We will replace this *Accepted Manuscript* with the edited and formatted *Advance Article* as soon as it is available.

You can find more information about *Accepted Manuscripts* in the [Information for Authors](#).

Please note that technical editing may introduce minor changes to the text and/or graphics, which may alter content. The journal's standard [Terms & Conditions](#) and the [Ethical guidelines](#) still apply. In no event shall the Royal Society of Chemistry be held responsible for any errors or omissions in this *Accepted Manuscript* or any consequences arising from the use of any information it contains.



Journal of Materials Chemistry B

Materials for Biology and Medicine

Full paper submission

Journal of Materials Chemistry B is a weekly journal in the materials field. The journal is interdisciplinary, publishing work of international significance on all aspects of materials chemistry related to biology and medicine. Articles cover the fabrication, properties and applications of materials.

2014 Partial Impact Factor of *Journal of Materials Chemistry B*: **4.726**
For more information go to www.rsc.org/materialsB

The following paper has been submitted to *Journal of Materials Chemistry B* for consideration as a **Full paper**.

Journal of Materials Chemistry B wishes to publish original research that demonstrates **novelty and advance**, either in the chemistry used to produce materials or in the properties/applications of the materials produced. Work submitted that is outside of these criteria will not usually be considered for publication. The materials should also be related to the theme of materials for biology and medicine.

Routine or incremental work, however competently researched and reported, should not be recommended for publication if it does not meet our expectations with regard to novelty and impact.

It is the responsibility of authors to provide fully convincing evidence for the homogeneity and identity of all compounds they claim as new. Evidence of both purity and identity is required to establish that the properties and constants reported are those of the compound with the new structure claimed.

Thank you for your effort in reviewing this submission. It is only through the continued service of referees that we can maintain both the high quality of the publication and the rapid response times to authors. We would greatly appreciate if you could review this paper in **two weeks**. Please let us know if that will not be possible.

Once again, we appreciate your time in serving as a reviewer. To acknowledge this, the Royal Society of Chemistry offers a **25% discount** on its books: <http://www.rsc.org/Shop/books/discounts.asp>. Please also consider submitting your next manuscript to *Journal of Materials Chemistry B*.

Best wishes,

Miss Ruth Norris
Managing Editor, *Journal of Materials Chemistry B*

Dr Fiona McKenzie
Executive Editor, *Journal of Materials Chemistry B*

Fabrication of electrospun poly (ethylene oxide)-poly (capro lactone) composite nanofibers for co-delivery of niclosamide and silver nanoparticles exhibits enhanced anti-cancer effects *in vitro*

*Poornima Dubey^a, P. Gopinath ^{*a,b}*

^aNanobiotechnology Laboratory, Centre for Nanotechnology,

^bDepartment of Biotechnology,

Indian Institute of Technology Roorkee, Roorkee, Uttarakhand-247667, India.

Corresponding author: Tel. +91-1332-285650; Fax. +91-1332-273560;

*E.mail: pgopifnt@iitr.ernet.in; gene gopi@gmail.com

Abstract:

An intrinsic property of many anticancer drugs including niclosamide is poor water solubility, which hindered their translation from laboratory to clinics. In an effort to enhance its water solubility and bioavailability, we have developed a simplistic strategies based on solvent evaporation and amorphous solid dispersions method. Among various solvent evaporation methods, electrospinning was adopted in the present work. Poly(ethylene oxide) (PEO) was selected as polymeric solid dispersion matrix of drug based on various advantageous properties of PEO. Moreover PEO could also serve as template for *in situ* synthesis of silver nanoparticles (Ag NPs). Furthermore the co-delivery of multiple anticancer drugs within nanocarrier is a promising approach to overcome the drug resistance and to achieve synergistic therapy. To achieve this goal, the drugs (niclosamide (nic) and, Ag NPs) were loaded separately and together (nic@Ag NPs) into the nanofiber. The as-prepared various formulations of composite nanofibers were well-characterized by different techniques. The *in vitro* release and kinetic studies suggest sustained release of niclosamide which followed Fickian diffusion kinetics. The anticancer potential of drug alone and the nic@Ag NPs loaded nanofibers were evaluated by MTT assay against A549 (lung carcinoma) and MCF-7 (breast carcinoma) cell lines. The co-delivery of anticancer drugs nic@Ag NPs from nanofiber displayed superior anticancer potential *in vitro* when compared to alone nic or Ag NP composite nanofibers. Additionally nic@Ag NPs showed better therapeutic efficacy against MCF-7 cells. To confirm the mechanism of cell death by nic@Ag NPs composite nanofiber on MCF-7 cells, various cell based assays were done. Our finding clearly explains that combination of drugs with diverse anticancer mechanism remarkably improved the therapeutic potential of drugs. Therefore, the nic@Ag NPs composite nanofiber as co-delivery system might have potential applications in combination cancer therapy.

Keywords: Silver nanoparticles, Niclosamide, Nanofibers, Drug delivery, Cancer therapy

Introduction

Since 50 years a well known FDA approved salicylanilide antihelminthic drug niclosamide (5-chloro-N-(2-chloro-4-nitrophenyl)-2-hydroxybenzamide) has been used against tapeworm infections. Beside that it was also used as a molluscicide for water treatment in schistosomiasis control programs. It has got renewed attention based on its antiviral effects against severe acute respiratory syndrome (SARS) virus, and anti-anthrax toxin properties [1]. In the recent past, numerous groups have separately explored the active role of niclosamide as a potential antitumor agent against diverse types of tumors [2-5]. Furthermore, niclosamide is a strong inducer of LC3-positive autophagosomes vesicle [6], an inhibitor of the Wnt/Frizzled [7], and mTOR signalling pathway [8]. It also uncouples mitochondrial oxidative phosphorylation [9], thus decreases the cell proliferation. Based on the diverse mechanism of action it provides negligible opportunity for acquired resistance over extended use. Thus it has been demonstrated as “old drug with new life”. Although the medical application of niclosamide is stalled due to its poor water solubility thus bioavailability [10]. The low aqueous solubility of the hydrophobic drug presents major hurdles for their *in vivo* administration. In addition, several anti-tumor drugs endure rapid removal from circulation and require specificity for cancer cells, mainly to declined efficacy and rigorous side effects [11]. Over the last decade, carrier based drug delivery systems such as, dendrimers, liposomes, polymer-drug complexes and micelles, have appeared as a new class of anticancer agents are at present under preclinical and experimental development as new nanomedicine that can transport a combination of multiple drugs to various cancers [12]. Micelles have been amongst the extensively explored classes of polymer assemblies, among which, a wide array of amphiphilic copolymers such as PEO poly (propylene oxide) [13], poly (ethylene oxide) (PEO)-poly (ϵ -caprolactone)[14], and PEO-poly (aspartic acid) [15] could utilized for the fabrication of drug delivery micelles, and many of them have been verified to provide

superior therapeutic efficacy *in vitro* and *in vivo*. At present, as many as fourteen polymer–drug conjugates gone through the scientific assessment and a polyglutamic acid (PGA)-paclitaxel conjugate (CT-2103, OPAXIO®, formerly known as Xyotax®) is likely to enter the marketplace in the very near prospect [15]. In March 2008, Cell Therapeutics agreed to a marketing approval function for OPAXIO® for the management of patients with NSCLC [15]. Recently few reports come up with an effort for improving water solubility of niclosamide by its encapsulation in polymeric nanoparticle such as PLGA, albumin and drug polymeric complex formation between niclosamide and PEI [16-17, 10].

PEO is a widely used polymeric matrix for solid dispersion to augment water solubility thus drug bioavailability. . Poly(ethylene oxide) (PEO) was selected as polymeric matrix for solid dispersion of drug to improve bioavailability of drug grafted into it due to its well known biocompatibility, high water solubility, and its stealthy properties *in vivo* in drug delivery applications. [18-20]. We have considered the inclusion of a drug into a water-soluble, biocompatible, biodegradable polymer PEO, under situation such that the drug is ended as amorphous compound. Moreover, a high surface area would aid in mass transfer and effective drug release. To accomplish this objective, electrospinning was applied [21]. Electrostatic spinning is a flexible polymer processing method in which a jet of a polymer solution or melt is focused to a high electric field ensuing in the formation of nanodimension fibers. The deposited fibers produced a nonwoven fabric, which can be used to a number of applications. The application of this tool to drug-based delivery systems has been studied only to a narrowed level. To produce drug delivery systems on the basis of this idea, a drug is included beside the polymer in the solution to be spun. Importantly, the high surface area coupled with nanofibers allow them for quick and effective solvent evaporation, which

provides limited time to the encapsulated drug to recrystallize supporting the generation of solid solutions or amorphous dispersions[21].

Although the polymer–drug conjugates are recognized for the delivery of a single therapeutic agent, but recently their utilization has been extended for the delivery of multi-agent therapy [15]. Based on the molecular complexity of several diseases, combination therapy is becoming more appropriate progressively for a improved long-term prospect and to reduce side effects. By and large the term ‘Combination therapy’ refers to the cure of a disease either by the concurrent incorporation of two or more pharmacologically active agents or the combination of diverse kind of therapeutics (e.g. chemotherapy and radiotherapy). Contrastingly to single-agent therapy, multi-agent therapy can alter various signalling pathways in diseased tissues, exploiting the therapeutic potential and, maybe overcome methods of resistance [15]. The utilization of combination therapy for tumor management is well recognized and for enhanced therapeutic efficacy combination antitumor treatment has extensively adopted in clinics. Although the chemotherapeutic medication are generally associated with rigorous side-effects, the administration of a combination of agents hitting diverse target molecules and exhibiting diverse toxicity profiles can advance the therapeutic index either in the form of better efficiency or in the form of similar efficacy and less toxicity.

The motivation for utilization of combination therapy is twofold. Firstly, when numerous drugs with diverse molecular targets are used, the cancer adaptation routes such as cancer cell mutations can be broken up. Second, when various drugs target the similar cellular pathway they could work together for higher therapeutic effectiveness and higher target specificity. Besides the combination chemotherapy, nanoparticle drug delivery has also shown

noteworthy assurance in cancer treatment. Collective therapy of two or more drugs encourages synergism among the diverse drugs against cancerous cells and suppresses drug resistance via separate mechanisms of action. Conversely nanoparticle drug delivery enhances the therapeutic efficacy and decreases the side effects of the drug payloads by increasing their pharmacokinetics [22]. Very recently these two dynamic research fields have been merged to further advances the efficacy of cancer therapeutics. Considering that Ag NPs has been added to the nanofiber as Ag NPs is well known for its anticancer potential at certain concentration [23-26]. Additionally, Ag NPs–polymer nanocomposites have been widely studied because of their potential advantages in various fields ranging from biosensing, electronic, optical, antimicrobial, anticancer, and tissue engineering applications. Generally, there are two possible approaches for synthesis of silver–polymer nanostructures the *in situ* and the *ex situ* approaches. In *ex situ* approach, Ag NPs were synthesised first followed by their addition into a polymer matrix [27]. The *in situ* approach involves Ag NPs synthesis within a polymer by reduction of silver ions into the polymerization matrix. Several polymers have been used such as nylon 6 matrix where electrospinning solvent of polymer formic acid solution acts as reducing agent, [28, 29] whereas other have followed both *in situ* and *ex situ* approaches [30]. Nonetheless along with random incorporation of Ag NPs inside and surface of the polymeric nanofibers, various researchers have adopted co-axial electrospinning where Ag NPs were the sheath and polymer serves as a core solution [31]. Various researchers have used polymer as stabilizing and reducing agent such as chitosan, and high molecular PEO etc [32, 25]. In our study, we have adopted the *in situ* approach for Ag NPs synthesis in PEO solution.

Along with development of drug resistance after tumor treatment, the local tumor recurrence after surgical intervention remains a major clinical challenge for most of the cancers.

Although chemotherapy or radiotherapy serves as adjuvant therapies after surgery for reduction of the chances of recurrence, but these therapies leads to severe side effects. Moreover, the repair and reconstruction of damaged tissue at the site of surgery is of great value for successful healing in several cancer therapies. Electrospun nanofibers have been widely used as localized drug delivery system with very hopeful preliminary results [33] due to their unique structural features and good drug loading capability. Several anticancer drugs such as paclitaxel [34] and doxorubicin [35] have been loaded into various nanofibers for postsurgical cancer treatment. But there is certain limitation of these scaffolds such as the development of tumor resistance, uncontrolled release of drug etc. Thus it is advantageous to design an implantable scaffold with enhanced anticancer efficacy and local drug delivery to avoid drug resistance by using combination therapy approach with controlled release system for long term healing. Such scaffold could also avoid any chance for cancer reoccurrence and further support the regeneration of damaged cells.

Thus the aim of our study was to explore anticancer potential of combination of drug-nanoparticle. Thus the first objective of the study was the generation of amphiphilic block composite copolymer nanofiber scaffold of poly (ethylene oxide)-b-poly (ε-caprolactone) (PEO-PCL) as carrier for the stabilization, solubilisation, and controlled delivery of niclosamide and explore the anticancer potential. Niclosamide-loaded PEO-PCL nanofibers were synthesized by a co-solvent evaporation method. The second objective of study was to incorporate the Ag NPs and drug together in polymeric matrix system and to investigate the effect of co-delivery of Ag NPs and drug by aid of nanofiber system for combination drug delivery system. This would be the first report for exploration of combination therapeutic effect of niclosamide with Ag NPs by using nanofiber based co delivery system.

Experimental:**Materials and methods:**

PEO (Mv.900,000), PCL (Mv.70,000–90,000), and niclosamide were purchased from Sigma-Aldrich, USA and used without any further modification. N, N-Dimethylformamide (DMF) and methylene chloride (DCM) and glutaraldehyde (25 vol %) were procured from Sisco Research Laboratories (SRL) Pvt. Ltd. India. Silver nitrate (AgNO₃; 99%) was obtained from Merck India. A549 cells (human lung adenocarcinoma) and MCF-7 (breast adenocarcinoma) cell lines were procured from National Centre for Cell Science (NCCS), Pune, India. The Dulbecco's modified Eagle's medium (DMEM) along with 10% FBS (Fetal bovine serum) and supplemented with 1% Penicillin-streptomycin was procured from Sigma Aldrich, USA and 7-dichlorofluorescein diacetate (DCFH-DA) was procured from Sigma Aldrich, USA.

Amorphous solid dispersion method for incorporation of niclosamide drug in PEO polymer:

PEO (3.5 wt %) and PCL (3 wt %) were suspended in a 4:1 v/v DCM–DMF solvent and combined to synthesize the solution for the electrospinning of the PEO–PCL blended nanofibers. 10mg niclosamide was dissolved in 1mL of DMF separately then the solution was added to PEO solution (4:1 v/v DCM–DMF). The niclosamide was completely dispersed in PEO matrix. The as-prepared solution was carried for electrospinning by mixing PCL solution (4:1 v/v DCM–DMF) into it and stirred for 2 h on magnetic stirrer to obtain complete homogenous solution.

***In situ* synthesis of Ag NPs and incorporation of nic@Ag NPs in PEO polymer matrix:**

In situ synthesis of Ag NPs were done in the PEO solution by the earlier explained scheme [25] which was then mixed individually with a PCL solution in a 4:1 v/v DCM–DMF solvent

blend and stirred for 1h for generation of homogeneous solution. For preparation of nic@Ag NPs-PEO solution separately prepared niclosamide-PEO and Ag NPs-PEO solution were mixed to obtain nic@Ag NPs-PEO blended solution. To obtain final solution for electrospinning PCL solution was mixed into it and stirred for 1h.

Electrospinning of niclosamide, Ag NPs and nic@Ag NPs composite nanofibers (Solvent evaporation and amorphous solid dispersion method):

Solvent evaporation and amorphous solid dispersion method was adopted for fabrication of water soluble drug encapsulated nanofiber. The electrospinning technique was used for the production of the nanofibrous mat. The fabrication of nanofibers were done in the occurrence of a high-voltage power delivery (8-14 kV) to the needle (18G) attached to a 2-mL syringe at a feeding rate of 0.6 mL/h forced through the syringe pump. The grounded electrode plate enclosed with aluminium foil by a thickness of 0.3-0.5 mm was utilized as a collector for nanofibers with a fixed straight distance from the needle tip (12– 14 cm). The electrospinning method was carried out under ambient temperature conditions (25 °C and 50-60 % relative humidity). The production of dried nanofibers was accomplished through electrospinning as volatile DCM solvent get evaporated easily from the polymeric solution while its way directed towards the collector, thus there was little requirement to dry the nanofibers. Additional drying of the nanofibers was completed in desiccators in the occurrence of silica for the complete removal of a residual solvent. The notation for the nanofibers was used as niclosamide, Ag NPs and nic@Ag NPs composite nanofibers. The optimized factors used for fabrication are concised as follows: 3.5 wt % PEO solution in a 4:1 v/v DCM–DMF solvent mixture, 3 wt % PCL, 10mg niclosamide and 1wt % of Ag NO₃. The 10 kV applied voltage for nic alone composite nanofiber, 12 kV for Ag NPs composite nanofiber and 12 kV for

nic@Ag NPs composite nanofibers, and 12 cm tip-to-collector distance, 0.5-1 mL/h solution flow rate, and 18 G blunt end tip needle.

Several factors such as voltage, solution viscosity, conductivity of solution, flow rate, tip to collector distance were optimized for the successful synthesis of the nanofibers. The solution viscosity is the critical factor determining the fiber morphology. It has been demonstrated that continuous and smooth fibers cannot be fabricated in very low viscosity solution, whereas very high viscosity makes the jet ejection hard from solution. Thus there is a need of optimized viscosity for electrospinning. Viscosity also depends on the molecular weight of polymer and polymer concentration in the solution. Thus we have used different ratios of polymers and optimized the viscosity as shown in (Fig. S2 (ESI[†])). Another important parameter is solution conductivity. Conductivity of alone polymer is poor as conductivity depends on the charge in the solution, but the addition of Ag NO₃ increases the conductivity of solution. The generation of a fluid jet depends on the occurrence of suitably high surface charge densities that are affected not only by the applied voltage, but also depends on the conductivity of the polymer dispersion. It is known that increase in conductivity means increase the charge in solution, thus more charges could pass by the electrospinning jet. The beaded fiber formation will occur if the solution is not fully stretched. Therefore, when a small amount of polyelectrolyte or salt is added to the solution, the increased solution conductivity will increase the stretching of the solution. Consequently, smooth fibers were formed which may otherwise yield beaded fibers. The increase in the stretching of the solution will also tend to yield fibers of smaller diameter [36]. Thus when compared to alone PEO-PCL blended nanofiber and nic composite nanofiber, the diameter of Ag NPs composite nanofiber and nic@Ag NPs composite nanofiber were less.

Physicochemical Characterization of the Nanofibers

Ultraviolet–Visible (UV–vis) Spectroscopic, Transmission Electron Microscopic (TEM) and X-Ray Diffraction (XRD) Analysis.

UV–vis spectral analysis was performed to confirm Ag NP formation and niclosamide incorporation into PEO solution (Hitachi UV–visible spectrophotometer). The size of particle the produced nanoparticles was confirmed with a TEM instrument (FEI Technai G2) function at an accelerating voltage of 200 kV. The sample preparation for TEM involved the deposition of as such synthesized nanofibers onto the non-carbon-coated copper TEM grids above the aluminium foil in the electrospinning chamber. The XRD analysis was done for the study of the crystallinity and nanoparticle distribution into the nanofibers. XRD patterns of the nanoparticle composite polymeric fibers was obtained by a Bruker AXS D8 Advance powder X-ray diffractometer (Cu K_{α} radiation) in the range of 20–90 °C at a scan speed of 0.05 °/min.

NMR and FTIR Analysis:

^1H NMR and C-13 NMR spectra of samples were recorded using Bruker 500 MHz nuclear magnetic resonance (NMR) spectrometer at 500.19 and 125.785 MHz resonance frequencies respectively. The NMR peak analysis and assignment were done in TOPSPIN software provided with NMR instrument. Tetramethylsilane (TMS) was utilized as an internal standard for calibration of chemical shifts (δ). Homogenous solution for NMR was made by dissolution of nanofibers in d_6 -DMSO in millimolar (mM) concentrations before experiments. FTIR analyses of samples were done using Thermo Nicolet FTIR spectrometer in the range 4000–400 cm^{-1} using KBr pellets.

Thermal Stability of Nanofibers:

The bulk compositional analysis of as-synthesized nanofibers was carried out by TG analysis. The nanofibers vulnerability to higher temperatures and consequence of drug and nanoparticle loading on the strength of nanofibers was understood from the thermograms acquired by TG analysis. Around 10 mg of respective polymeric nanofiber were heated from 32 °C to 400 °C at a constant rate of 10 °C/min in EXSTAR TG/DTA 6300. A constant nitrogen atmosphere was maintained throughout the TG analysis of all samples. Various phases of weight loss in the thermogram were confirmed with degradation of specific components of the drug loaded nanofibers.

Contact Angle Measurement:

Static contact angles on nanofiber plane were calculated using the sessile drop method with Drop Shape Analysis System-DSA30 (Krüss, Hamburg, Germany). 30 µL of deionized water was dropped on top of desiccated nanofiber at 37°C and the contact angle was measured after 60 s of incubation time in order to avoid discrepancy in contact angle measurement due to position and time. Various nanofibers formulations were used in this study, (i.e. bare PEO-PCL nanofibers, nic composite nanofibers, Ag NPs composite nanofiber and nic@Ag NPs composite nanofibers) to study the effect of drug and nanoparticle incorporation by contact angle.

In Vitro Drug Release Study:**Release study of niclosamide from nic composite nanofiber**

The drug loaded nanofibers was cut into small pieces of ~10 mg weight. After drying, nanofiber was placed in PBS solution. The amount of drug released was estimated after various time points (0 h-20 days for nic@Ag NPs composite nanofibers) by measuring the

absorbance (Hitachi UV–vis spectrophotometer) of the released medium (i.e. PBS pH 7.4) at 340 nm for niclosamide. The experiment was done in triplicate. The calibration curve was plotted for niclosamide for estimation of the amount of drug released from the nanofibers. The release study was carried out at 37°C at 100 rpm in orbital incubator shaker. To explore the drug release kinetics various kinetic models observed as mentioned in Table S1 (ESI†).

$$\% \text{ Release} = [\text{Conc. of drug aliquot} \times \text{volume of release medium} / \text{initial drug conc.}] \times 100$$

Release study of Ag from nic@Ag NPs and Ag NPs composite nanofibers:

To examine the release profile of Ag NPs and nic@Ag NPs composite nanofibers the nanofibers were cut into small pieces of ~10 mg weight. The amount of Ag ions released from Ag alone and nic@Ag NPs composite nanofibers after incubation at various time points (0 h -100 h) were measured using AAS in the graphite furnace method (Avanta M, GBC Scientific Equipment) using pure Ag (1, 2, 4 ppm) standards as reference. The amount of drug release from the nanofiber was estimated for 0 h-20 days by measuring the absorbance (Hitachi UV–vis spectrophotometer) of the release medium (i.e. PBS pH 7.4) at 340 nm for niclosamide.

Cell Culture

The human cancer cell lines were selected for this study, including A549 cells and MCF-7 cells which were acquired from National Centre for Cell Sciences (NCCS), Pune, India. The cell lines were maintained in Dulbecco's modified Eagle's medium (DMEM, Sigma-Aldrich) supplemented with 10% (v/v) Fetal bovine serum (FBS) and 1% penicillin-streptomycin solution (Sigma -Aldrich, USA) at 5% CO₂ in a humidified incubator at 37°C.

In vitro* Cellular Studies:*Cytotoxicity assay of niclosamide, Ag NPs and nic@Ag NPs composite nanofiber**

MTT colorimetric assay was adopted to quantitate the anticancer potential of niclosamide, Ag NPs and nic@Ag NPs composite nanofibers. Two human cancer cell lines were selected for the study of anticancer effect of drug and nanoparticle alone and their combined effect. All the formulations of nanofibrous mats including control nanofiber, niclosamide, Ag NPs, nic@Ag NPs composite nanofibers were deposited on 12 mm round glass dishes to maintain the uniformity of deposition weighing 1.65 mg, each of them were loaded with the predefined fixed amount of drug. The nanofiber dishes were kept in wells of 24 well plate and then UV-sterilized for 45 min. The cells were seeded over these nanofibers at a seeding rate of 5000 cells/ well for cell viability assay. The experiment was carried out all the four formulations of nanofiber in time dependent manner for 24 h, 48 h respectively independently in triplicates. In brief, before taking 24-well plate for microplate readings, the solubilised formazan crystals were transferred to free wells in order to avoid interference of nanofibers. The obtained absorbance was normalized with respective reference values and correlated with positive controls to arrive at percentage cell viability. Similarly, an independent MTT assay was carried out for estimating the efficacy of drug loaded nanofibers against MCF-7 at two time points i.e. 24 h, 48 h.

$$\% \text{ Cell Viability} = [A_{570} \text{ treated}/A_{570} \text{ control}] \times 100$$

Microscopic Methods for Observation of Cellular Morphology Changes:**Acridine Orange-Ethidium Bromide (AO-EB) staining**

AO-EB staining was done to observe the time dependent apoptosis induction in cells seeded over nic@Ag NPs composite nanofibers. After incubating the cells for particular time period over nic@Ag NPs composite nanofibers (i.e. 6, 12, 48, 96 h) cell were stained with 2-3 μL of

AO-EB blend (10 $\mu\text{g}/\text{mL}$ working concentration) to screen the apoptotic cells. The cells were incubated at 37°C with dyes for 10-15min and then given PBS wash to remove the excess dyes (to avoid background fluorescence of free dye). The cellular morphology was then examined under EVOS cell imaging system (life technologies, USA) and images were recorded under blue filter, green filter and transmitted mode. Similarly, Hoechst 33342 and rhodamine B staining was also used to observe nuclear and cytoplasmic changes occurred during apoptosis (Fig. S5).

FE-SEM Analysis of Cell Morphology

The cells were seeded over glass cover slips coated with nic@Ag NPs composite nanofibers. Cells were treated for 24 h, than the treated cells were washed twice with PBS and then fixed with 2% glutaraldehyde for 10min followed by 20%, 40%, 60% and 80% ethanol gradient fixation. The sample was then air dried at 37°C . The fixed cells were then sputter coated with gold for examination of cell membrane integrity under FE-SEM.

Determination of intracellular Reactive Oxygen Species (ROS) generation by niclosamide, Ag NPs and nic@Ag NPs composite nanofiber:

MCF-7 cells were seeded on nanofibers placed in 6 well plate for 3-6 h. Cells were then harvested by trypsin-EDTA and cell pellet was collected in DMEM medium. To remove nanofiber any further the cell pellets were further centrifuged to obtain cell pellets without DMEM medium. The nanofiber treated cell pellets were then resuspended and incubated with 200 μL of PBS including 20 μM DCFH-DA and for 20 min incubated at 37°C . The DCFH-DA is non fluorescent dye employed to measure ROS action inside the cell. After entering into the cell by diffusion the acetate groups of dye get cleaved by intracellular esterases found within the cells and DCFH-DA get transformed to the highly fluorescent 2, 7-

dichlorofluorescein (DCF) leading oxidation [37]. DCF has excitation and emission maximum at 495 nm and 529 nm, correspondingly. Directly following incubation, treated samples were observed for DCF fluorescence utilizing a flow cytometer (Amnis Flowsight). The software utilized for analysis was Amnis Ideas which measure the obtained information for 10,000 events/sample and ROS production was measured in terms of population of cells with green (DCF) fluorescence.

Gene expression analysis by semi-quantitative reverse transcriptase-polymerase chain reaction (RT-PCR):

For differential gene expression study of apoptotic signaling genes MCF-7 cells (2×10^6 cells/mL in 6 well plate) were grown for 24- 48 h over nic@Ag NPs composite and control nanofibers. Beta-actin (b-actin) (housekeeping gene) was exploited as an internal control. Complete RNA from MCF-7 cells was isolated by utilizing Tri reagent (Sigma Aldrich, USA) and cDNA was prepared by reverse transcription of denatured RNA (1 μ g) by using M-MLV reverse transcriptase at 37°C for 50min in reaction mixture of 20 μ L. The human apoptotic genes primer sequence used in the study are mentioned in Table S2 (ESI†). The semi quantitative PCR was performed by using gene specific upstream and downstream primers. The PCR reaction cycle steps were as follows; an initial denaturation (94°C for 5 min) was followed by a cycle of denaturation (94 °C for 60 s), annealing (60 °C for 60 s), and extension (72 °C for 30 sec) with a final extension (72 °C for 10 min). Ultimately the PCR products were resolved in 1.2 % agarose gel and envisaged by ethidium bromide staining under UV light in gel documentation unit (Biorad). Image lab 4.0 software provided with gel doc unit was used for analysis of the fold difference in the gene expression between control and treated samples.

Statistical analysis

The results are mentioned as mean \pm S.D. for all the separate experiments. The data were examined by two-way ANOVA or Student's t test either valid, using GraphPad Prism 6.0, or statistically significant value are indicated by $*p < 0.05$, $**p < 0.005$, and $***p < 0.001$.

Result and discussion:

Incorporation of niclosamide, Ag NPs and nic@Ag NPs drugs in PEO polymer matrix by amorphous solid dispersion methods:

The idea of common solvent was used for dissolution of drug in polymer matrix as both are soluble in DCM and DMF at 4:1 ratio. The incorporation of drug in polymer matrix has been checked by TEM and drug release in PBS which was confirmed by UV visible spectroscopy as showed in Fig.1a and Fig. S1 (ESI[†]). The successful incorporation of drug into polymer matrix has been further confirmed by FTIR and NMR analysis. The ¹H-NMR spectrum of drug alone and drug in PEO has been studied and found the disappearance of certain peaks when compare to alone. Hydrogen bonds among the CONH amide group of niclosamide and the ether oxygen of PEO are the expected basis for the high miscibility between niclosamide and PEO. Such drug-polymer molecular interactions aid in dispersion of niclosamide into amorphous stage of PEO ensuing in high molecular mobility of niclosamide in the mixture that leads to improved dissolution rate of niclosamide in aqueous media. The disappearance of NH peak in proton NMR of complex showed interaction of niclosamide with PEO as shown in Fig.1d (as shown in Table S3, Fig S3 (ESI[†])). Similarly the drug peak in PEO matrix showed disappearance of characteristic IR peaks (as mentioned in Table S4 (ESI[†])) when compared to bare niclosamide drug peaks also showed in Fig.1c. Naive niclosamide drug is significantly more hydrophobic when compared to drug incorporated in PEO matrix. Furthermore the transformation of drug from crystalline to amorphous phase was confirmed

by DTA analysis (Fig.4) which showed enhanced solubility and stability thus better drug delivery therapeutics of formulation. Further confirmation of enhanced drug hydrophilicity was attributed to wettability analysis by contact angle measurement which clearly showed better hydrophilicity of nic composite nanofiber when compared to bare nanofiber or niclosamide drug alone as showed by Fig.5. Stabilization of the drug loaded polymeric matrix was achieved by its blending with PCL a hydrophobic polymer.

In the recent past, we have reported the *in situ* synthesis and incorporation of Ag NPs into the high molecular weight PEO polymeric solution [25]. In this method, we have tried out synthesis of Ag NPs into high molecular weight PEO solution [38] (where DMF act as co-solvent for dissolution of PEO) which was reported to reduce and stabilize Ag NPs completely. In this synthesis method we have utilized idea of partial reduction of Ag NO₃ by DMF followed by its complete reduction and stabilization by PEO solution. In many fabrication methods various toxic chemicals has been utilized either as cross linking or reducing agents which hampered the therapeutic potential of nanofibers. In our study thus we have followed the *in situ* synthesis of Ag NPs inside the nanofibers during the electrospinning process without the use of any external cross linking or reducing agents. Thus the current as-prepared nanofibers proved to be better therapeutic nano platform for future anticancer application (25).

To the above synthesized Ag NPs solution, the already prepared niclosamide dispersion in PEO matrix was mixed. The same solution was electrospun for fiber fabrication by solvent evaporation method to obtain amorphous solid dispersion. The optical properties of the Ag NPs and niclosamide in PEO solution were studied. Niclosamide showed characteristic peak at 340 nm whereas the plasmon absorption peak of Ag NPs came around 395 nm (Fig.1a)

The result of UV-vis showed small size nanoparticle which was further confirmed by TEM analysis (Fig S1a (ESI†)). The diameter of Ag NPs came out to be 11.6 nm in diameter as explained by histogram (Fig S1b (ESI†)). The Ag NPs were present on the surface of nanofiber apart from being their inside incorporation. Thus surface of nanofiber was rough when compared to the alone PEO-PCL nanofiber. This was further supported by the release study, as the initial burst release showed around 15% of Ag NPs release which demonstrate that hydrophilic PEO stabilized Ag NPs composite were also distributed onto the surface which leads to their initial rapid dissolution from nanofiber surface after water contact. The crystallinity and structural characteristics of the Ag NPs in the PEO composite nanofibers were investigated by the powder XRD method. The X ray diffraction spectral patterns obtained were observed by PaNalytical X'Pert High Score Plus software. The typical peaks of elemental Ag were shown at $2\theta = 37.99, 44.2, 64.53, \text{ and } 77.28$ corresponds to the Ag (111), Ag (200), Ag (220), and Ag (311), respectively and the above four miller indices diffraction peaks were in concurrence with JCPDS 040783 (Fig 1b). The XRD spectral patterns established that the polymeric blend was semicrystalline and also established the presence of Ag as Ag^0 in Ag NPs in the composite nanofibers, where the crystalline arrangement of Ag was a surface cubic crystal arrangement.

Physicochemical Characterization of the Nanofibers

Microscopic and Spectroscopic interpretation of the Nanofibers

FE-SEM images of the niclosamide, Ag NPs and nic@Ag NPs composite nanofibers are shown in fig. 2b-d. The diameter analysis of nanofiber was done by Image J software. The alone PEO-PCL polymer nanofibers were found to be 150–300 nm in diameter as reported earlier [25], while the nanofibers incorporated with Ag NPs were around 122nm in diameter, as shown in Fig 2b in inset by histogram. The nic composite nanofiber were found to be

870nm diameter (Fig. 2c) and nic@Ag NPs composite nanofiber were found to be 632nm in diameter which was shown in Fig. 2d in inset by histogram. The nanofibers showed rough surface when compared to the alone PEO-PCL nanofibers which showed that drug and Ag NPs were not only integrated into the fiber but were also located on the surface of the nanofibers. The TEM image undoubtedly showed the incorporation of drug and Ag NPs on the surface and inside the polymeric nanofiber matrices (Fig S1 (ESI[†])).

FTIR Spectroscopic Measurement

The typical FTIR spectrum of the PEO-PCL nanofiber and various composite nanofibers such as niclosamide, Ag NPs and nic@Ag NPs have been shown in the Fig. S4 (ESI[†]). The FTIR analysis provides a major insight into the interaction of amide with hydrophilic polymeric matrix PEO which ultimately leads to enhancement of solubility of drug which was also supported by contact angle and DTA data. The major IR peaks of niclosamide alone and niclosamide in nanofiber has been shown in Table.S4 (ESI[†]). The comparative peak analysis has been shown between niclosamide alone and niclosamide incorporated in nanofiber. Various modes of interactions are possible between drug and polymer. Niclosamide traverse into the microenvironment of hydrophobic core of the polymeric hydrophobic part (PCL) whereas hydrophilic part of polymer PEO aid into the solubility enhancement of drug. The probable reason for conversion of drug from crystalline to amorphous phase may include the interaction of -CHO group of PEO with niclosamide -NH group and -OH by hydrogen bonding and electrostatic interactions.

As earlier we have reported the plausible reason behind the formation of Ag NPs in PEO solution would be the incomplete reduction of Ag⁺ ions by the occurrence of the aldehyde group (-CHO) in PEO and presence of DMF molecules in solution. The ion-dipole or

electrostatic interaction of the electron-rich oxygen atom of hydroxyl (-OH) and -CHO group with electropositive Ag^+ ions. We have observed the presence of all the major peaks for PEO and PCL solutions but for alone PEO-PCL nanofiber the major peaks were either shifted or absent in composite nanofibers. The C-H stretching vibration peak was observed at 2876 cm^{-1} , CH_2 scissoring mode was present at 1466 cm^{-1} , whereas the CH_2 wagging mode was present at 1360 and 1341 cm^{-1} , CH_2 twisting mode was present at 1279 cm^{-1} , C=O=C stretching was present at 1104 cm^{-1} . Nevertheless, the semicrystalline stage of PEO was confirmed by the occurrence of a triplet peak of C=O=C stretching vibrations at 1145 , 1095 , and 1059 cm^{-1} , with the maximum intensity at 1095 cm^{-1} got disappeared along with the peak at 2876 cm^{-1} in solution following the synthesis of Ag NPs in the PEO matrix [39].

Thermal Stability of Nanofibers

TGA and DTA analysis:

The thermal stability of the various samples was analyzed by thermogravimetric analysis (TG) under N_2 atmosphere, from room temperature to 400°C at a heating rate of $10^\circ\text{C min}^{-1}$. Fig.3 and 4 showed the TGA and DTA curves of the naive PEO-PCL nanofibers and various composite nanofibers including nic, Ag NPs and nic@Ag NPs composite nanofibers, respectively. Compared with the TGA curves of alone PEO-PCL nanofiber, composite nanofibers showed difference in their thermal stability. When compared to bulk niclosamide drug and naive PEO-PCL nanofiber, nic composite nanofiber showed better thermal stability, the thermal degradation of niclosamide starts around 200°C and 230°C whereas for the nic composite nanofiber degradation starts after 300°C as shown in Fig. 3a, b. The Ag NPs and nic@Ag NPs composite nanofiber decomposes early before 200°C (Fig 3c) in contrast to alone PEO-PCL nanofiber which could be due to thermal conductivity of Ag NPs in composite nanofibers [25]. The comparative thermal analysis has been shown for various

formulations in Fig 3a-d. This weight loss indicates evaporation or thermal decomposition in the material. The weight loss of nic nanofiber was more than niclosamide drug as shown in Fig 3b, could be due to high surface area of nanofiber and in nic@Ag NPs further decrease could be attributed to the presence of Ag NPs which could increase the thermal conductivity of the composites, as seen in Fig. 3c, d. The slight weight loss was due to the loss of moisture and trapped water, DCM and DMF solvent in the electrospun composite nanofibers while the major weight loss was due to the combustion of drug and nanoparticle incorporated composite organic PEO-PCL matrix.

Niclosamide is a well known hydrophobic drug for which we have tried to improve solubility by its incorporation into the polymer matrix of high molecular weight hydrophilic semi-crystalline PEO polymer. While preparing the formulation two considerations need to be taken care; solubilization of the drug molecule in a polymer matrix to evade the rate-limiting phase-to-phase solubilisation step and production of steady supersaturated systems to endow with the chemical potential for drug release from the amount formulation [40]. In our synthesis approach we have considered these variables through the use of solid solution/dispersion techniques by using PEO polymer and electrospinning approach [41, 42]. By carrying a drug into a polymeric carrier matrix, it is dissolved/dispersed denoting that the crystal lattice energy has previously been surmounted which was confirmed by DTA analysis. The DTA analysis of drug alone showed exothermic peak around 225°C which confirmed that alone drug is crystalline in nature Fig.4. However the drug incorporated into polymer matrix as in the nic composite nanofiber, showed absence of this exothermic peak illustrating the amorphous nature of drug incorporated into the polymer matrix. Nevertheless presence of one small exothermic peak around 70°C was due to the semi-crystalline nature of base polymeric blend (PEO-PCL) nanofiber as showed from arrow in outlet of Fig (4a,b).

The polymeric endothermic peak shifts in nic composite nanofiber towards higher temperature range around 380°C which further substantiate the further decrease in crystallinity of polymer by drug incorporation. This showed increase in amorphous nature of drug in nanocomposite formulation. Although the crystallinity of polymer got decreased but it is sufficient to act as drug carrier as shown by our controlled release study and also supported by literature.[43] Along with the nic composite nanofiber, the Ag NPs and nic@Ag NPs composite nanofiber also showed presence of one small exothermic peak as shown in Fig 4a, b attributed to semi-crystalline nature of base polymeric blend nanofiber carrier. Thus the above synthesised nanofiber drug delivery system provide better therapeutic efficacy. This bi-component semi-crystalline copolymer has been recently explored by researchers independently as controlled drug delivery system for water insoluble drugs. [44] Thus our study is in agreement with previous studies of this polymeric blended composite nanofiber as controlled-release delivery systems for water insoluble drugs.

Wettability Analysis by Contact Angle Measurement

The wettability analysis of biomaterial is essential parameters as biomaterials may come in contact with various biological fluids during biomedical applications. [32]. It is advantageous to check the hydrophilicity of scaffolds when one aims to produce materials scaffolds for cellular attachment proliferation and, skin tissue engineering. Surface hydrophilicity of scaffold could be measured by water contact angle and surface tension. Surface tension (γ) is a straight measurement of intermolecular force upon the surface. The biomaterial surface roughness (or topography) is an additional important factor affecting cell adhesion and proliferation behaviour. Undeniably, roughness modulates the biological response of cells in contact with the scaffold. The relationship between surface roughness and wettability was

defined by Wenzel in 1936 that showed that adding surface roughness will enhance the wettability caused by the certain chemistry of the surface.

Thus measurement of water contact angle is a recognized method to study surface homogeneity, changes in surface composition, and wettability (i.e. hydrophilicity and hydrophobicity). It gives a clear thought regarding the characteristics of the scaffold surface, whether it could be hydrophilic or hydrophobic. We have checked the contact angle among a liquid and the surface of the electrospun matrix by using sessile drop casting method. We have used polymeric blend of PEO-PCL as nanofiber base for composite synthesis thus the contact angle measurement was done for all the formulations. The contact angle got significantly decreased for composite nanofiber when contrast to alone PEO-PCL nanofiber as shown in Fig. 5. The contact angle of nic composite nanofiber got decreased after drug incorporation into hydrophilic and hydrophobic polymeric blend nanofiber which showed increased hydrophilicity of drug (Fig.5) by its incorporation which is in agreement with DTA data (Fig. 4). This could be attributed to topographical change in the nanofiber by enhanced surface roughness of nanofiber due to the fact that while electrospinning drug reside both inside and at the surface of nanofiber in consistent with our previous study. (25) The hydrophilicity of nanofiber further got increased by incorporation of Ag NPs into nic@Ag NPs composite nanofiber. The reason for this increase in hydrophilicity of scaffold could be the further increase in surface roughness of nanofiber by addition of Ag NPs. Another probable reason could be the release of Ag^+ ions from Ag NPs by oxidation in the aqueous phase, might simultaneously get adsorbed onto the Ag NPs surface in the development of hydrated Ag^+ ions as consistent with previous reports [25]. Thus our study suggests the suitability of the designed scaffold based on increase in hydrophilicity. It also suggests that

the change in surface topography plays important role and can affect contact angle and wettability.

Drug Dissolution and Release Kinetics Studies

The drug release profile and kinetic studies have been shown in Fig 6A, B. There was distinct release profile for drug and nanoparticle released from nic, Ag NPs and nic@Ag NPs composite nanofiber once come in contact with hydrophilic environment. The drug and nanoparticle both showed initial burst release around 15% and 18% respectively which could be due to surface adhered particles and initial rapid dissolution of PEO polymer as shown in Fig. 6A. The initial rapid phase was followed by slow controlled release of nanofiber which could be around 43% for drug and 50% for nanoparticle in 20 days and 100 h respectively (Fig. 6A (a, b)). For both drug and nanoparticle discrete events determine the release kinetics which includes the degradation of semicrystalline polymers in two stages. There could be surface and bulk degradations are two distinctive forms of degradation. The first stage involves the aqueous phase mixing into the amorphous regions with arbitrary hydrolytic scission of labile bonding of PEO ether bonds as they are prone to hydrolysis or enzymatic degradation. The second stage is where the most of the amorphous regions were degraded. Thus diffusion and dissolution of hydrophilic polymeric matrix PEO took place during the release mechanism (Fig 6A). Water is a key factor throughout the hydrolytic event and thus water intrusion into the scaffold is of noteworthy importance for the study of release and degradation kinetics. Thus diffusion and dissolution is the key player of drug release mechanism and the schematic presentation of drug release from various composite nanofibers has been shown in Fig. 6A c. As niclosamide became amorphous in the hydrophilic polymeric matrix and thus better miscible into the hydrophilic polymer PEO as supported by DTA, NMR, FTIR studies, this further enhance the delivery therapeutics of drug in a

controlled manner. The rate controlling event in the release was dissolution as the drug was embedded in the erodible matrix. The dissolution event involves two transport processes, i.e. water diffusion and polymer chain disentanglement.

Various mathematical models have been measured for studying drug release profile of niclosamide. Amongst them the Higuchi model was based on the hypothesis that system is diffusion controlled in one dimension which was governed by Fick's law of diffusion. But in our system along with diffusion, dissolution was also equally possible, thus there could be possibility of non-Fickian mass transfer which cannot be ruled out. Another model called Hixson-Crowell model which hypothesised that although dissolution occurs but the dissolution takes place in planes that are parallel to the drug surface. Thus possibility of this model was also excluded. Thus the choice of model was Korsmeyer-Peppas which was based on a straightforward relationship which illustrates the drug discharge from a polymeric system

$$M_t / M_\infty = Kt^n$$

Where M_t / M_∞ is a fraction of drug released at time t , n is the release exponent and k is the release rate constant. The n value is used to distinguish diverse release for cylindrical shaped matrices.

This model categorised released methods based on the value of n exponent. For the case of cylindrical arrangement, $0.45 \leq n$ the model matches to a Fickian diffusion mechanism, if the value lies between $0.45 < n < 0.89$ it is considered as non-Fickian mass transport mechanism. [47]. In order to study the release kinetics, data acquired from *in vitro* drug release studies were plotted as log cumulative percentage drug release versus log time. Thus the release

mechanism was considered based on the n value acquired for the Korsmeyer-Peppas model fitting curve. For finding out the n value one should consider portion of release curve which have $M_t / M_\infty < 0.6$. Our release profile showed value of n less than 0.45 for drug in both the conditions with Ag NPs and alone in nanofibers as shown in Fig. 6B, which showed clearly it followed Fickian diffusion mechanism. The regression (R^2) values found for each model indicates the significance of the given model for the niclosamide drug release as shown in Fig. 6B.

In vitro cellular studies

Investigation of growth inhibition by nic@Ag NPs composite nanofibers.

***In vitro* cytotoxicity assay of nic@Ag NPs composite nanofiber**

The *in vitro* cytotoxicity of nic@Ag NPs nanofibers was tested against both MCF-7 and A549 cells by the colorimetric MTT assay as shown in Fig 7a,b. The niclosamide and Ag NPs are drugs ingredient of composite nanofiber, displayed growth inhibition in a time and concentration dependent manner (Fig. 7). Nic@Ag NPs nanofibers induces synergistic cell death at less concentration when compare to alone niclosamide and Ag NPs. The IC_{50} value of nic and Ag NPs composite nanofibers against A549 cells and MCF-7 cells after 48h were found to be 1.45 μ M, 6.5 μ g/mL and 1.39 μ M, 4.7 μ g/mL respectively whereas the IC_{50} value of nic@Ag NPs composite nanofibers against A549 cells and MCF-7 cells were found to be 1.24 μ M and 1.21 μ M respectively. Thus the results indicate enhanced effect of nic@Ag NPs against both cell lines when compare to alone nic or Ag NPs. composite nanofiber.

Study of Cell Morphology:

Acridine Orange-Ethidium Bromide (AO-EB) Staining

AO-EB staining is well-known for visualization of nuclear changes and apoptotic body formation that are typical of programmed cell death (apoptosis). It is considered as a principle method for distinguishing apoptotic cells from necrotic ones. As Ag NPs and niclosamide both kills cell primarily by means of apoptosis. So in order to understand the manner of cell death by nic@Ag NPs composite nanofiber the cells treated by nanofibers were stained with fluorescent dyes AO-EB and examined under fluorescent microscope. The AO being a vital dye stains equally live and dead cells whereas EB stains cells which lost their membrane integrity (dead cells). As AO imparts green color fluorescence by permeating the nuclei of cells thus live cells appear green as shown in Fig. 8a. The mechanism behind the green fluorescence is binding of dye to the double stranded DNA by getting intercalated. The treated cells were stained differentially when compare to control cells. Control cells were uniformly green, whereas treated cells showed various stages of cell death such as the early apoptotic cells stains green and carried bright green dots in the nucleus as outcome of chromatin condensation and nuclear disintegration as shown in Fig. 8b The late apoptotic cells allow permeation of EB thus appears in orange red color fluorescence as shown in Fig.8c-f. The mechanism behind the red orange fluorescence of EB is again the binding with double stranded DNA in intercalation mode. Contrarily to necrotic cells late apoptotic cells illustrates condensed and fragmented nuclei, whereas the necrotic cells showed nuclear morphology resembling live cells with no chromatin condensation. The cells treated with only niclosamide or only Ag NPs showed less orange red fluorescence when compared to green owing to more early apoptotic cells at IC_{50} concentration whereas cells treated with nic@Ag NPs composite nanofiber showed more late apoptotic cells due to more number of cell death which resulted in permeation of more EB into the cells and thus more orange red fluorescence. Thus the dual staining substantiates significantly more number of cell deaths by nic@Ag NPs composite nanofibers.

Cell Morphology Analysis by FE-SEM:

The FE-SEM images of cells seeded over control nanofibers showed cell growth and proliferation (Fig. S3 ESI) whereas the cells seeded over nic@Ag NPs nanofiber clearly showed distinctive morphology of control and treated cells. On both nic@Ag NPs treated and control nanofibers treated cells, the cells were able to grow properly over polymeric nanofibers PEO-PCL where the cells hold their intact morphology and proper cell attachment. The nic@Ag NPs treated cells showed change in the morphology characteristics of apoptotic cells after 24 h of treatment such as formation of apoptotic bodies, membrane blebbing, cell degeneration and lysis. Fig. 9a, b clearly showed normal and treated cell morphology which in corroboration with AO-EB staining confirms the event of apoptosis in treated cells whereas control nanofibers support the growth and proliferation of cells.

Intracellular ROS Generation

The intracellular generation of hydrogen peroxide, was measured by the DCFH-DA method, an indirect method for quantifying ROS. In this study the intracellular ROS generation was substantially higher in nic@AgNPs treated MCF-7 cells than alone niclosamide and Ag NPs treated cells. ROS generation was measured to examine the possible role of oxidative stress as a primary mode of nic@AgNPs induced toxicity. Interestingly ROS generation induces cellular stress which ultimately leads to cell death by either of two separate pathways, through apoptosis and necrosis [48, 49]. Although Ag NPs alone and niclosamide alone has already been reported for induction of ROS [50].

The induction of oxidative stress by contact of nanoparticles with mammalian cells leads to the cellular ROS generation crossing the cellular antioxidant defences. Even though the distinct mechanism is not understood yet, but the critical role of ROS in nanoparticle-

mediated genotoxicity and cytotoxicity has been reported by several researchers [51]. In the present study, for exploration of the effect of nic@Ag NPs composite nanofiber on the cellular ROS generation, the nanofiber treated cells were inspected under microscope for their capacity to produce green fluorescence of DCF, formed by the intracellular oxidation of DCFH-DA dye. The rise in the ROS generation in the nic@Ag NPs was clearly evident (Fig 10) in treated cells contrast to the untreated cells. The increase in ROS concentration in treated cells was monitored by examining the population of cells with increased green fluorescence in a flow cytometer. It was apparent from the flow cytometric analysis (Fig 10d) that nic@Ag NPs increased the level of intracellular ROS when compare to alone nic and Ag NPs at their respective IC_{50} values as shown in Fig.10a-d.

Gene Expression Analysis

Mitochondria cell death pathway induced in ROS dependent manner:

Programmed cell death or apoptosis is a gene regulation event, which is necessary equally for physiological and pathological conditions. In order to corroborate the stimulation of the apoptotic signalling pathway by nic@AgNPs induced ROS generation, the expression of various apoptotic genes were semi-quantitatively measured through RT-PCR [52]. All the gene expression was standardized with the level of the housekeeping gene b-actin expression (Fig. 11a, b). The chief regulatory mechanisms of apoptosis comprises mitochondrial responses and Bax (bcl-2-associated X protein), death receptors, activation of caspases, and the regulation of Bcl-2 (basal cell lymphoma 2)) gene expression [23]. Nic@Ag-NPs induced highest activation of caspase-3 and apoptosis, which might divulge the mitochondrial apoptotic cell death pathway. As our finding demonstrate the expression of Bax and Bcl-2 gene expression could be synchronized in a different way by Ag-NPs, which proposed that a steadiness in the expression of these genes and proteins may be drawn in in the organization

of the apoptosis process. Caspase-3 and 9 (cysteine-dependent aspartate-directed proteases) are components of the cysteine protease family, which was recognized as major controller of programmed cell death apoptosis. These enzymes are implicated not only in the beginning but also in the completing stage of apoptosis by chopping as much as 400 substrates [53]. Their cleavage provokes the majority of the distinctive morphological and biochemical transformations in apoptotic cells, such as DNA fragmentation, chromatin condensation and cell shrinkage. Gurunathan et al. estimated the possible toxicity of biologically produced Ag-NPs in MDA-MB-231 human breast cancer cells [54]. They designated an enhanced level of caspase-3 activation in the treated cells. This result coincides with our finding. We found manifold increase in expression of the caspases that are central initiators or effectors in the cell death pathways as shown in Fig. 11a, b. As ROS target mitochondria and cause apoptosis and DNA damage [50] thus our data clearly support mitochondrial mediated apoptotic pathway induction by nic@Ag NPs composite nanofiber.

Along with caspase various other factors such as pro-apoptotic genes such as tumor suppressor gene p53, Bax and cmyc expression was also up-regulated substantially which further confirms the DNA damage event due to generation of stress in ROS mediated manner in the cell. Whereas down-regulation of the anti-apoptotic genes such as bcl-xl (basal cell lymphoma-extra large) and bcl2 was observed. The increase in p53 gene expression by niclosamide and Ag NPs was strongly supported by previous literature [10, 23] In the occurrence of DNA damage or cellular stress, p53 activate cell-cycle arrest to give time for the damage to be repaired or for self-mediated apoptosis [54, 55]. The enhanced expression of pro-apoptotic gene Bax further pave a way for mitochondrial outer membrane permeabilization (MOMP) and oligomeric pore formation for release of cytochrome c. It leads to trigger of caspase 3 which ultimately results in caspase 3 mediated apoptosis. A

schematic presentation of apoptotic induction in ROS mediated manner was shown in Fig. 11c. Thus the use of different drugs which targets different cell death pathway enhances the therapeutic effect at low dosage. Thus this formulation of nic@Ag NPs composite nanofiber further aid in understanding of using nanoparticle and drug for better cancer therapy.

Conclusion

In summary, we have tried to enhance the water solubility of sparingly water soluble anticancer drug niclosamide by its solid dispersion in PEO polymer matrix using solvent evaporation/amorphous solid dispersion approach. The nanofiber provides better surface area for drug release and mass transfer. The drug loaded nanofiber showed better hydrophilicity than drug alone which was confirmed by contact angle measurement. The reason behind that could be the conversion of crystalline drug into amorphous state based on its dispersion in hydrophilic PEO polymer matrix. The amorphous nature of drug was further confirmed by DTA analysis which clearly showed absence of endothermic peak in spectrum of drug loaded in nanofiber. The enhance in solubility by increase in amorphous nature is due to the higher Gibbs free energy in the amorphous state than the more stable crystalline state. In our study, we have explored the possibility of the combination of the water insoluble anticancer drug niclosamide with Ag NPs for cancer therapy. It was found that drug showed sustained and controlled release followed by initial burst release from both drug alone loaded and nic@Ag NPs loaded nanofibers. Further to enhance the therapeutic efficacy of drug, it was combined with Ag NPs and found that combined effect (nic@Ag NPs) of both showed better antitumor potential against A549 and MCF-7 cells than their individual effect (niclosamide or Ag NPs composite nanofiber). To explore the mechanism behind cell death, ROS assay was done which showed enhanced ROS by nic@Ag NPs composite nanofiber as compared to alone niclosamide and Ag NPs composite nanofibers. To further understand the molecular

mechanism we have done semi-quantitative RT-PCR analysis which showed the increase in pro-apoptotic genes with highest expression of caspase and decrease in anti-apoptotic genes. The highest expression of caspase is correlated to mitochondria mediated apoptotic cell signalling. The Ag NPs are known to exhibit ROS mediated cell death and niclosamide is known to inhibit cell death by various other pathways. Thus the combined effect resulted in enhanced therapeutic effect of dual drug nanofiber (nic@Ag NPs composite nanofiber). The combination of anticancer drugs with diverse pharmacological action has emerged as a capable therapeutic strategy in the treatment of cancers. Our scaffold showed better cell adhesion and proliferation which could help in cell regeneration. Thus it can serve as post surgical implant to avoid any chance for cancer reoccurrence at localized tumor site with enhanced anticancer effect with control release system for long term healing and with minimum chance for drug to acquire resistance against it. Taken together; our study demonstrated that nic@Ag NPs composite nanofiber based combination therapy holds significant potential towards the cancer therapeutics.

Acknowledgements:

This study was supported by the Science and Engineering Research Board (no. SR/FT/LS-57/2012) and the Department of Biotechnology (no. BT/PR6804/GBD/27/486/2012), Government of India. PD is thankful to the Ministry of Human Resource Development, Government of India, for the fellowship. Sincere thanks to Department of Chemistry and Institute Instrumentation Centre, IIT Roorkee for the various analytical facilities provided.

References:

1. A. Jurgeit, R. McDowell, S. Moese, E. Meldrum, R. Schwendener and U. F. Greber, *PLoS Pathog.*, 2012, **8**.

2. T. Ye, Y. Xiong, Y. Yan, Y. Xia, X. Song, L. Liu, D. Li, N. Wang, L. Zhang, Y. Zhu, J. Zeng, Y. Wei and L. Yu, *PLoS One*, 2014, **9**.
3. A. I. Londoño-Joshi, R. C. Arend, L. Aristizabal, W. Lu, R. S. Samant, B. J. Metge, B. Hidalgo, W. E. Grizzle, M. Conner, A. Forero-Torres, A. F. Lobuglio, Y. Li and D. J. Buchsbaum, *Mol. Cancer Ther.*, 2014, **13**, 800–11.
4. R. C. Arend, A. I. Londoño-Joshi, R. S. Samant, Y. Li, M. Conner, B. Hidalgo, R. D. Alvarez, C. N. Landen, J. M. Straughn and D. J. Buchsbaum, *Gynecol. Oncol.*, 2014, **134**, 112–120.
5. Y. Li, P. K. Li, M. J. Roberts, R. C. Arend, R. S. Samant and D. J. Buchsbaum, *Cancer Lett.*, 2014, 349, 8–14.
6. A. D. Balgi, B. D. Fonseca, E. Donohue, T. C. F. Tsang, P. Lajoie, C. G. Proud, I. R. Nabi and M. Roberge, *PLoS One*, 2009, **4**.
7. M. Chen, J. Wang, J. Lu, M. C. Bond, X. R. Ren, H. K. Lyerly, L. S. Barak and W. Chen, *Biochemistry*, 2009, **48**, 10267–10274.
8. B. D. Fonseca, G. H. Diering, M. A. Bidinosti, K. Dalal, T. Alain, A. D. Balgi, R. Forestieri, M. Nodwell, C. V. Rajadurai, C. Gunaratnam, A. R. Tee, F. Duong, R. J. Andersen, J. Orłowski, M. Numata, N. Sonenberg and M. Roberge, *J. Biol. Chem.*, 2012, **287**, 17530–17545.
9. J. Cunarro and M. W. Weiner, *Biochim. Biophys. Acta*, 1975, **387**, 234–240.
10. S.U. Kumar, P. Gopinath, *Colloids Surf B Biointerfaces.*, 2015, **131**, 170–81.
11. J. L. Arias, *Mini-Reviews in Medicinal Chemistry*, 2011, **11**, 1–17.
12. J. H. Lee and A. Nan, *J. Drug Deliv.*, 2012, **2012**, 1–17.
13. G. S. Kwon, M. Yokoyama, T. Okano, Y. Sakurai and K. Kataoka, *J. Control. Release*, 1994, **28**, 334–335.
14. W. Zhang, Y. Shi, Y. Chen, J. Hao, X. Sha, and X. Fang, *Biomaterials*, 2011 **32**, 5934–5944.
15. F. Greco and M. J. Vicent, *Adv. Drug Deliv. Rev.*, 2009, **61**, 1203–1213.
16. Meng-Yi Bai, Hui-Ching Yang. *Colloids and Surfaces A: Physicochem. Eng. Aspects*, 2013, **419**, 248–256.
17. B. Bhushan, P. Dubey, S. U. Kumar, A. Sachdev, I. Mataia and P. Gopinath, *RSC Adv.*, 2015, **5**, 12078.
18. J. M. Harris, N. E. Martin and M. Modi, *Clin. Pharmacokinet.*, 2001, **40**, 539–551.

19. R. B. Greenwald, C. D. Conover and Y. H. Choe, *Crit. Rev. Ther. Drug Carrier Syst.*, 2000, **17**, 101–161.
20. M. L. Nucci, R. Shorr and A. Abuchowski, *Adv. Drug Deliv. Rev.*, 1991, **6**, 133–151.
21. J. Doshi and D. H. Reneker, *Conf. Rec. 1993 IEEE Ind. Appl. Conf. Twenty-Eighth IAS Annu. Meet.*, 1993.
22. C. M. J. Hu, S. Aryal and L. Zhang, *Ther. Deliv.*, 2010, **1**, 323–334.
23. P. Gopinath, S. K. Gogoi, P. Sanpui, A. Paul, A. Chattopadhyay and S. S. Ghosh, *Colloids Surfaces B Biointerfaces*, 2010, **77**, 240–245.
24. P. Dubey, I. Matai, S.U. Kumar, A. Sachdev, B. Bhushan, P. Gopinath, *Adv Colloid Interface Sci.* 2015, 221:4-21.
25. P. Dubey, B. Bhushan, A. Sachdev, I. Matai, S.U. Kumar, P. Gopinath, *J. Appl. Polym. Sci.* 2015, 132, 42473.
26. P. Gopinath, S. K. Gogoi, A. Chattopadhyay and S. S. Ghosh, *Nanotechnology*, 2008, **19**, 075104.
27. R. Thomas, K. R. Soumya, J. Mathew, E. K. Radhakrishnan. *Appl Biochem Biotechnol* 2015, **176**, 2213–2224.
28. Q. Shi, N. Vitichuli, J. Nowak, J. Noar, J. M. Caldwell, F. Breidt, M. Bourham, M. McCord, X. Zhang, *J. Mater. Chem.* 2011, **21**, 10330–10335.
29. J. Song, H. Kang, C. Lee, S. H. Hwang, J. Jang. *ACS Appl. Mater. Interfaces* 2012, **4**, 460–465.
30. C-L. Zhang, S-H. Yu, *Chem. Soc. Rev.* 2014, **43**, 4423.
31. M.M.G. Fouda, M.R. El-Aassar, S. S. Al-Dey. *Carbohydr. Polym.* 2013, **92**, 1012–1017.
32. D-G. Yu, J. Zhou, N. P. Chatterton, Y.Li, J. Huang, X. Wang. *Int.J.of Nanomed.* 2012:7 5725–5732.
33. K. Qiu, C. He, W. Feng, W. Wang, X. Zhou, Z. Yin, L. Chen, H. Wang, X. Mo, *J. Mater. Chem. B*, 2013, **1**, 4601–4611.
34. G. P. Ma, Y. Liu, C. Peng, D. W. Fang, B. J. He, J. Nie, *Carbohydr. Polym.* 2011, **86**, 505–512.
35. F. Y. Zheng, S. G. Wang, M. W. Shen, M. F. Zhu and X. Y. Shi, *Polym. Chem.*, 2013, **4**, 933–941.
36. H. F. Hong, S. Jeong. *J. of Nanosci. and Nanotech.* 2010,**10**, 1–5.

37. P. Sanpui, A. Chattopadhyay and S. S. Ghosh, *ACS Appl. Mater. Interfaces*, 2011, **3**, 218–228.
38. C. D. Saquing, J. L. Manasco, S. A. Khan, *Small*, 2009, **5**, 944–951.
39. A. Ahmad, M. Y. A. Rahman and M. S. Suait, *J. Appl. Polym. Sci.*, 2012, **124**, 4222–4229.
40. K. T. Savjani, A. K. Gajjar and J. K. Savjani, *ISRN Pharm.*, 2012, 2012, 1–10.
41. C. Leuner and J. Dressman, *Eur. J. Pharm. Biopharm.*, 2000, **50**, 47–60.
42. A. T. M. Serajuddln, *J. Pharm. Sci.*, 1999, **88**, 1058–1066.
43. M-K. Park, S. Jun, I. Kim, S-M. Jin, J-G. Kim , T. J. Shin, E. Lee. *Adv. Funct. Mater.* 2015, **25**, 4570–4579.
44. M. V. Natu, H. C. de Sousa, M.H. Gil. *Int.J. of Pharmaceutics*. 20103, **97**, 50–58.
45. W. Cui, X. Li, S. Zhou and J. Weng, *Polym. Degrad. Stab.*, 2008, **93**, 731–738.
46. U. Stachewicz, A.H. Barber. *Langmuir* 2011, **27**, 3024–3029.
47. S. Dash, P. N. Murthy, L. Nath and P. Chowdhury, *Acta Pol. Pharm.*, 2010, **67**, 217–23.
48. M. Jeyaraj, M. Rajesh, R. Arun, D. MubarakAli, G. Sathishkumar, G. Sivanandhan, G. K. 49. Dev, M. Manickavasagam, K. Premkumar, N. Thajuddin and A. Ganapathi, *Colloids Surfaces B Biointerfaces*, 2013, **102**, 708–717.
49. S.U. Kumar, I. Matai, P. Dubey, B. Bhushan, A. Sachdev, P. Gopinath. *RSC Adv.*, 2014, **4**, 38263–38272.
50. S. L. Lee, A. R. Son, J. Ahn and J. Y. Song, *Biomed. Pharmacother.*, 2014, **68**, 619–624.
51. K. Kang, H. Jung and J. S. Lim, *Biomol. Ther.*, 2012, **20**, 399–405.
52. M. J. Akhtar, M. Ahamed, S. Kumar, M. M. Khan, J. Ahmad and S. a Alrokayan, *Int. J. Nanomedicine*, 2012, **7**, 845–57.
53. J. Baharara, F. Namvar, T. Ramezani, N. Hosseini and R. Mohamad, *Molecules*, 2014, **19**, 4624–4634.
54. S. Gurunathan, J. W. Han, V. Eppakayala, M. Jeyaraj and J. H. Kim, *Biomed Res. Int.*, 2013, **2013**.
55. J. E. Choi, S. Kim, J. H. Ahn, P. Youn, J. S. Kang, K. Park, J. Yi and D.-Y. Ryu, *Aquat. Toxicol.*, 2010, **100**, 151–159.

List of Figures

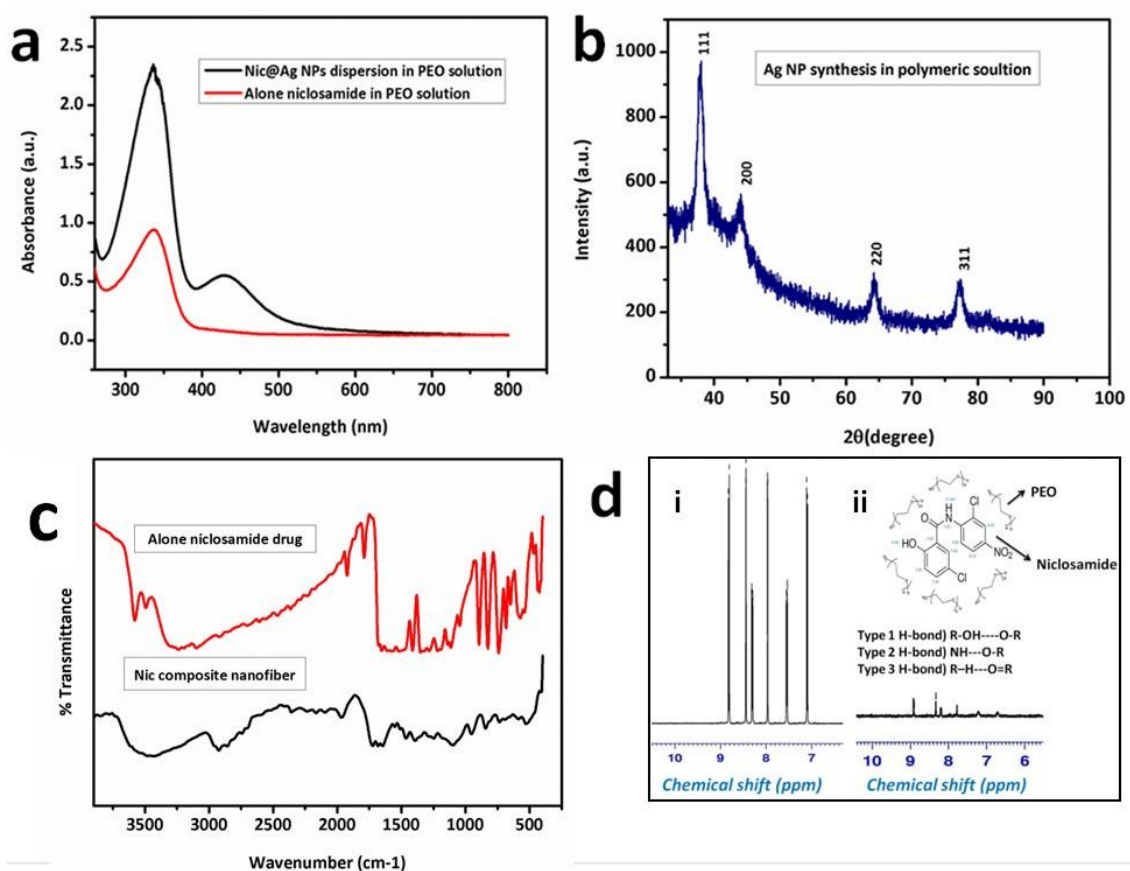


Figure.1 a) UV-visible spectroscopic analysis of alone niclosamide and nic@Ag NPs dispersion in PEO solution, respectively b) Characteristic XRD pattern of the as-synthesized Ag NPs in PEO polymeric solution. c) FTIR analysis of naive drug and nic composite nanofiber. d) ¹H NMR spectral analysis of alone niclosamide drug and nic composite nanofiber.

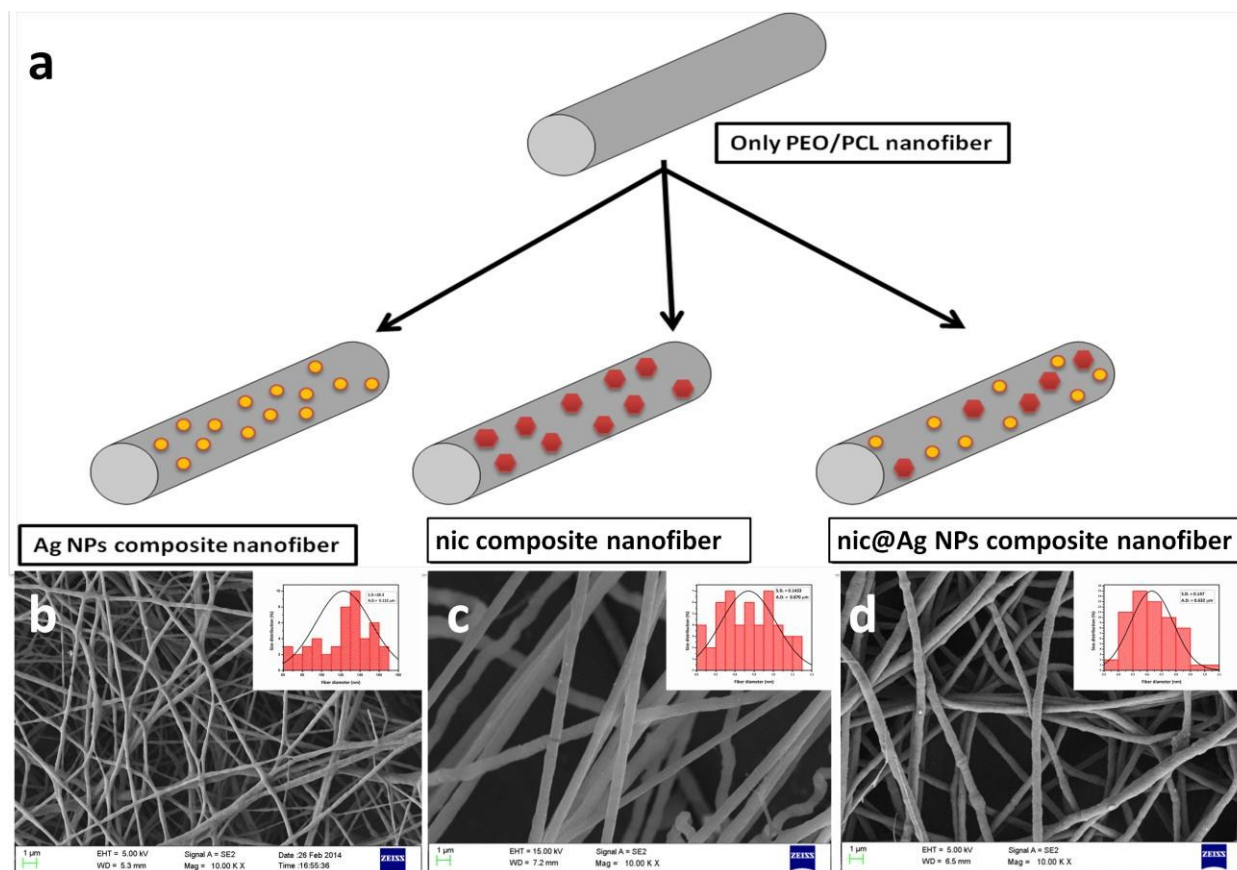


Figure.2 a) Schematic representation of backbone nanofiber scaffold and various composites formulated from it. b) FE-SEM micrographic observation of Ag NPs, nic and nic@Ag NPs composite nanofiber *Scale Bar 1 μ m*. (b-d) The insets showing diameter distribution histogram of respective nanofibers.

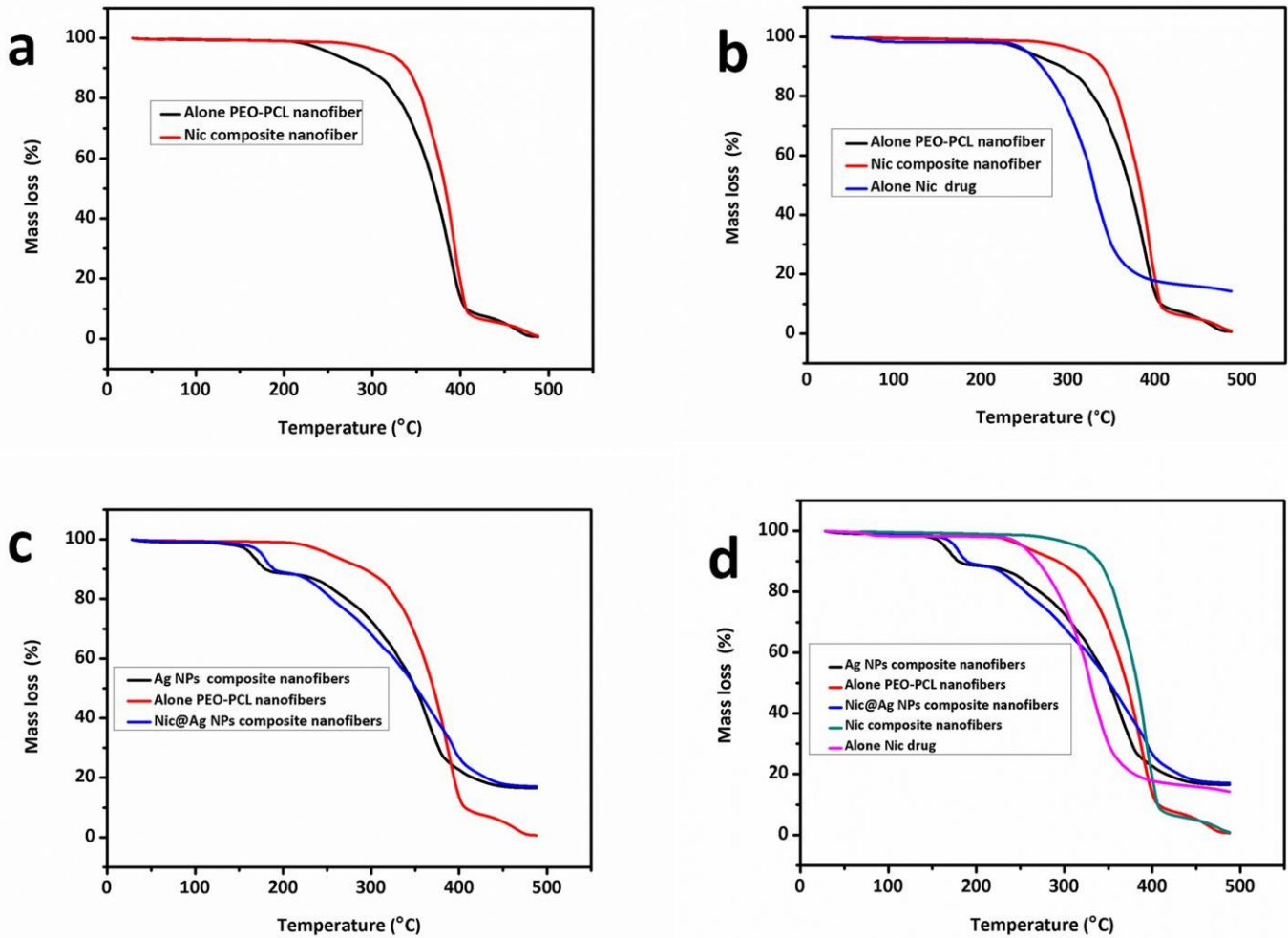


Figure.3 a) Thermo gravimetric analysis (TGA) of various formulations of composite nanofibers (a-d).

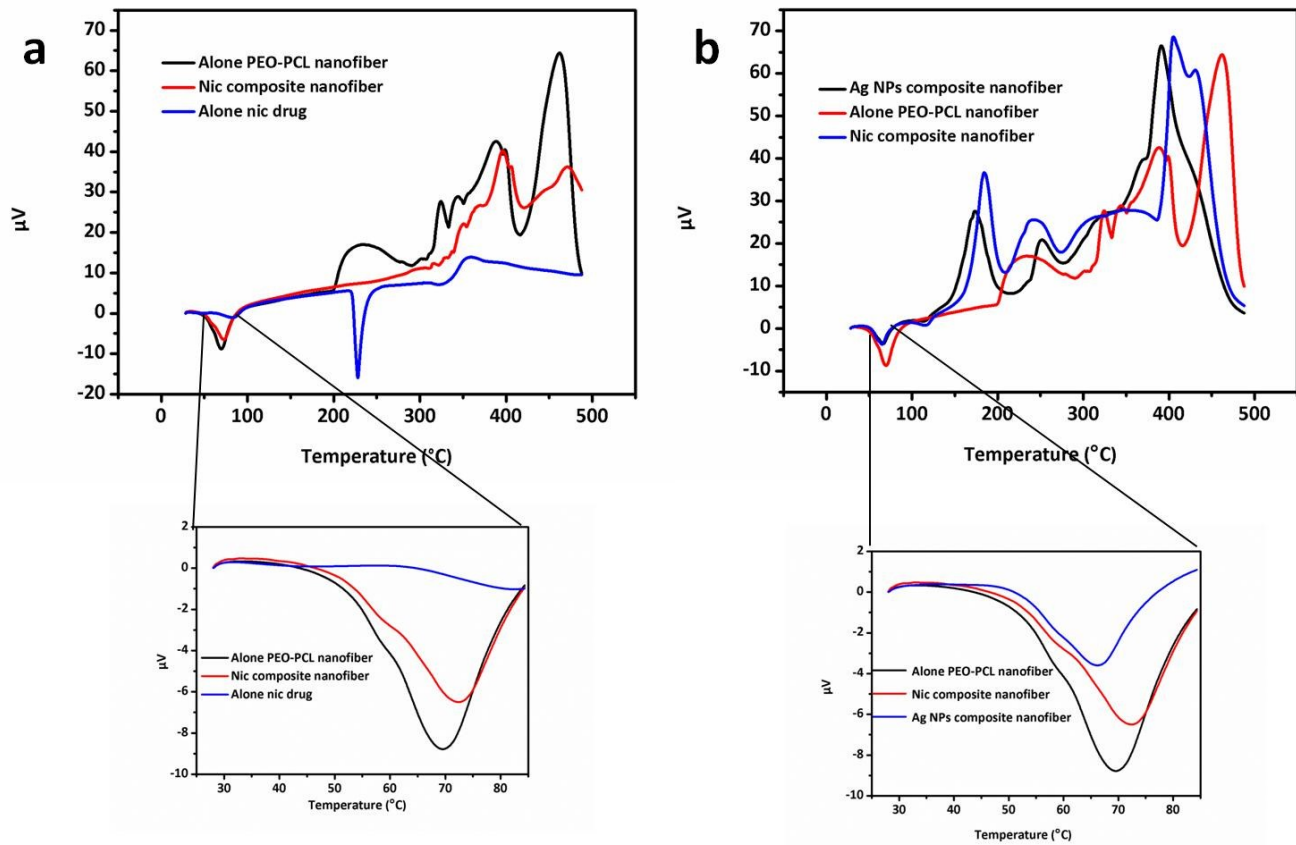


Figure.4 DTA analysis of various formulations of composite nanofibers (a, b). The outlet showed the small region from 30-100 $^{\circ}\text{C}$ for both a,b and marked by line.

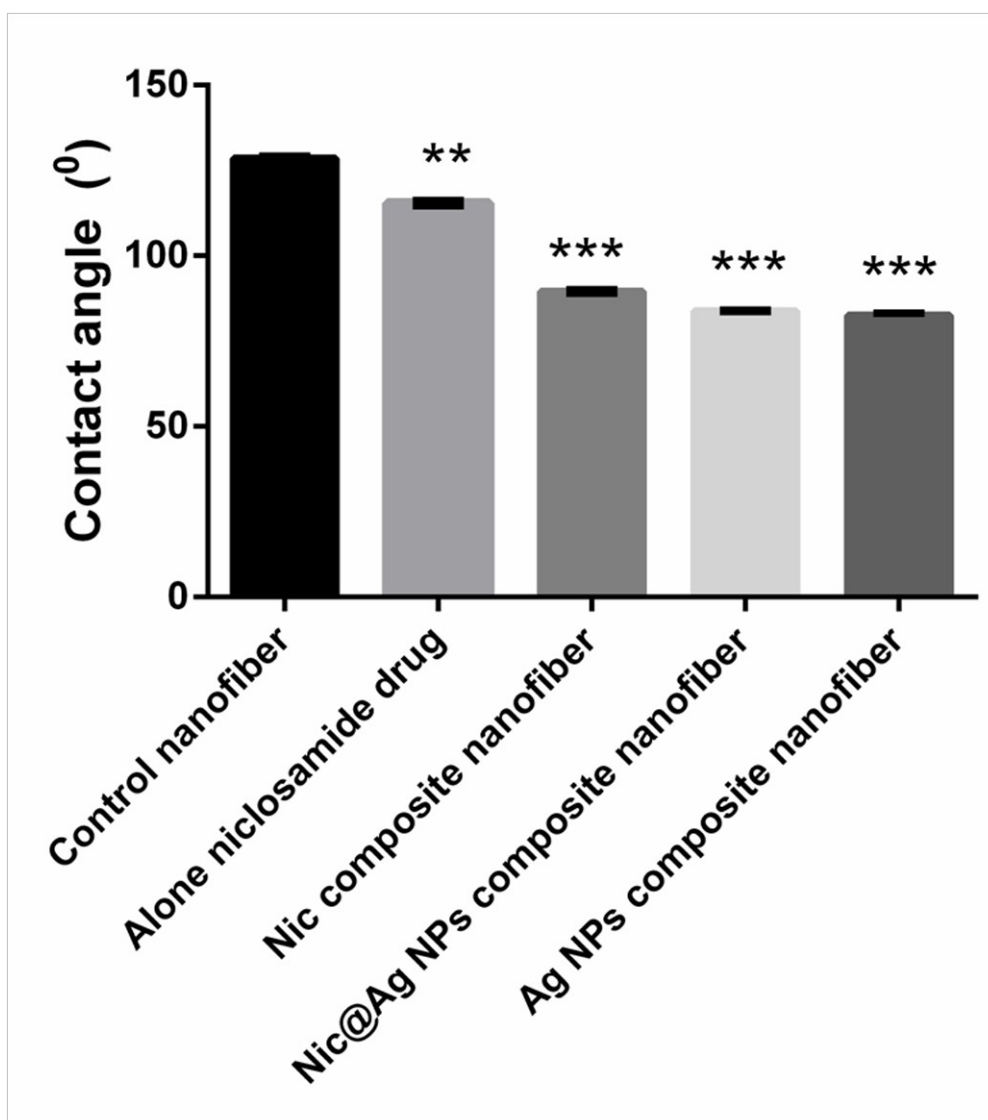


Figure.5 Wettability analyses of various nanofiber membranes by drop casting method are plotted as histogram and significance was measured from control nanofiber. The student t-test was performed to obtain level of significance from control nanofibers. Statistical significance between various groups were denoted by $*p < 0.05$, $**p < 0.005$, $***p < 0.001$.

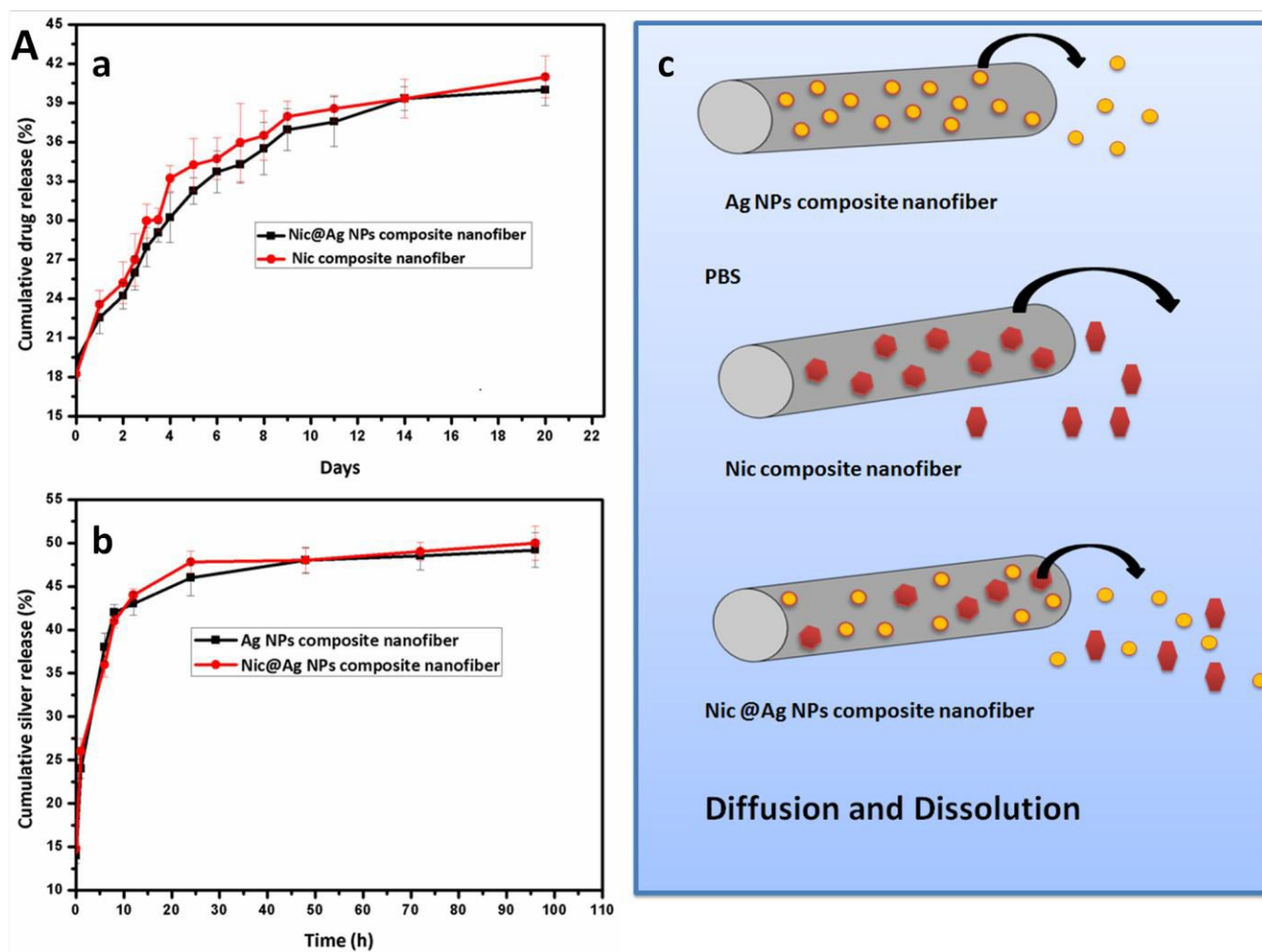


Figure.6A a) Cumulative drug release profile of drug released from drug alone and nic@Ag NPs composite nanofiber. b) Ag NPs release profile from alone Ag NPs and nic@Ag NPs composite nanofiber. c) Schematic illustration of drug release from various composite nanofibers.

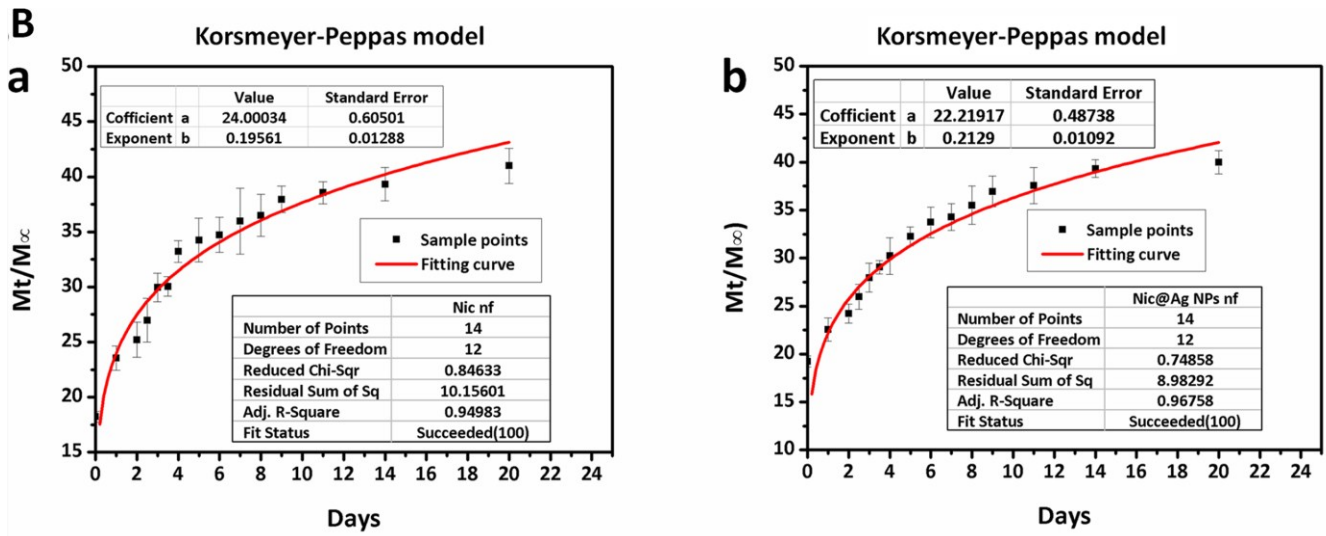


Figure.6B Drug release kinetic model fitting curve done by Korsmeyer-Peppas model for alone drug loaded and nic@Ag NPs composite nanofiber.

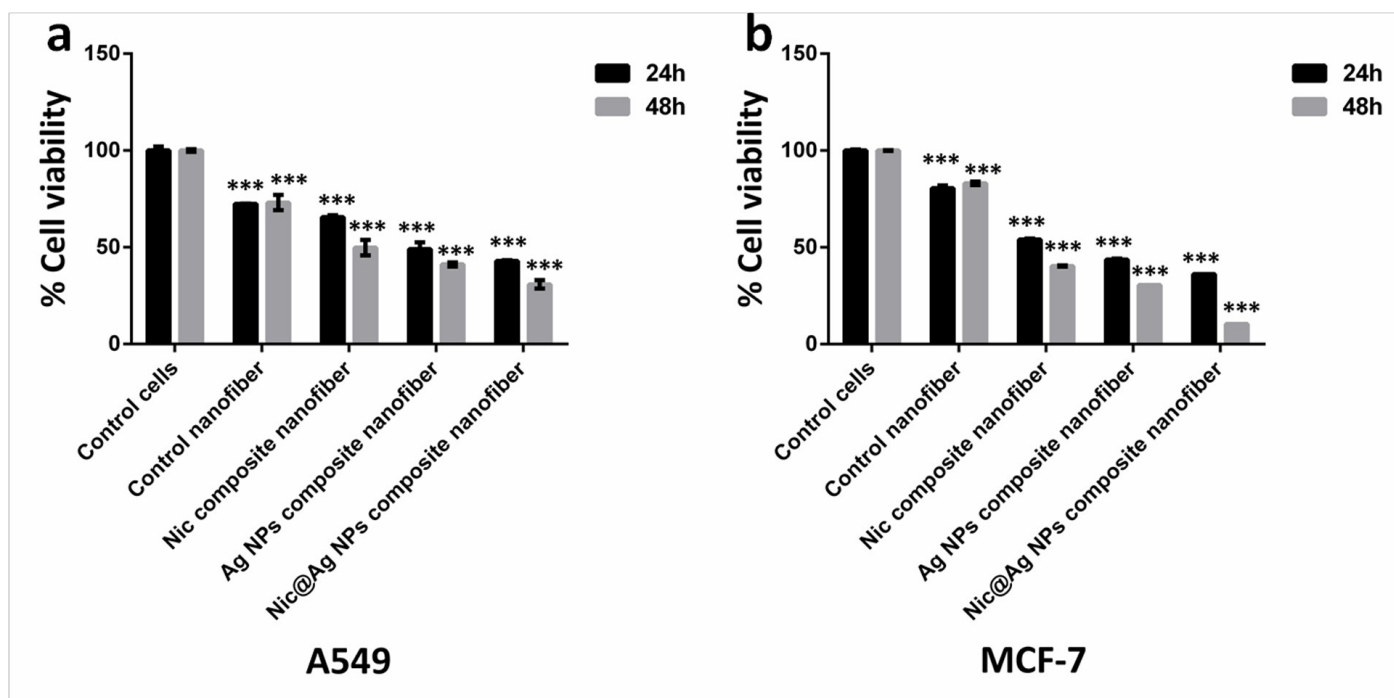


Figure.7 Cell viability assay (MTT assay) after seeding A549 lung carcinoma cells and MCF-7 breast carcinoma cells on various nanofibers for different time points (24 h and 48 h). Two way ANOVA was done to establish multiple comparison between groups. The values are shown as mean \pm S.D. (n=2). Statistical significance between various groups were denoted by * $p < 0.05$, ** $p < 0.005$, *** $p < 0.001$.

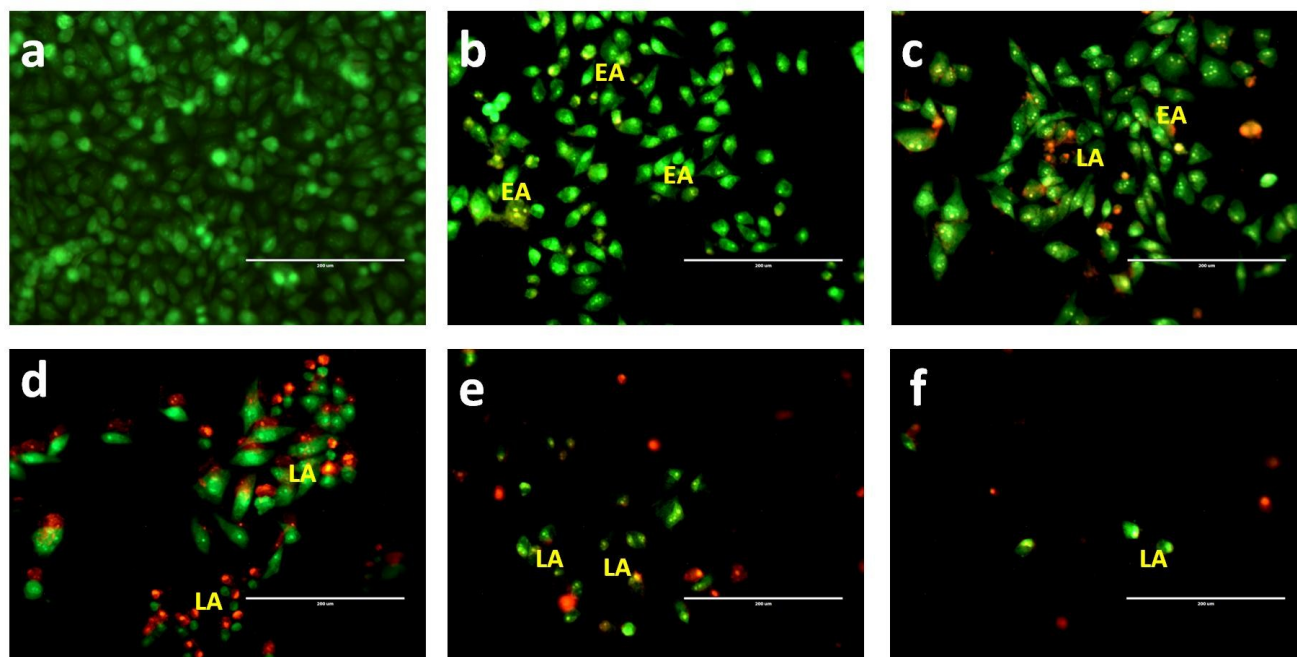


Figure.8 AO-EB dual stained images of MCF-7 cells seeded over control and nic@Ag NPs composite nanofibers for different period of time (6 h, 12 h, 24 h, 48 h, 96 h) as shown in images a-f respectively. Notation EA and LA corresponds to early and late apoptosis, respectively. Scale bar 200 μ m.

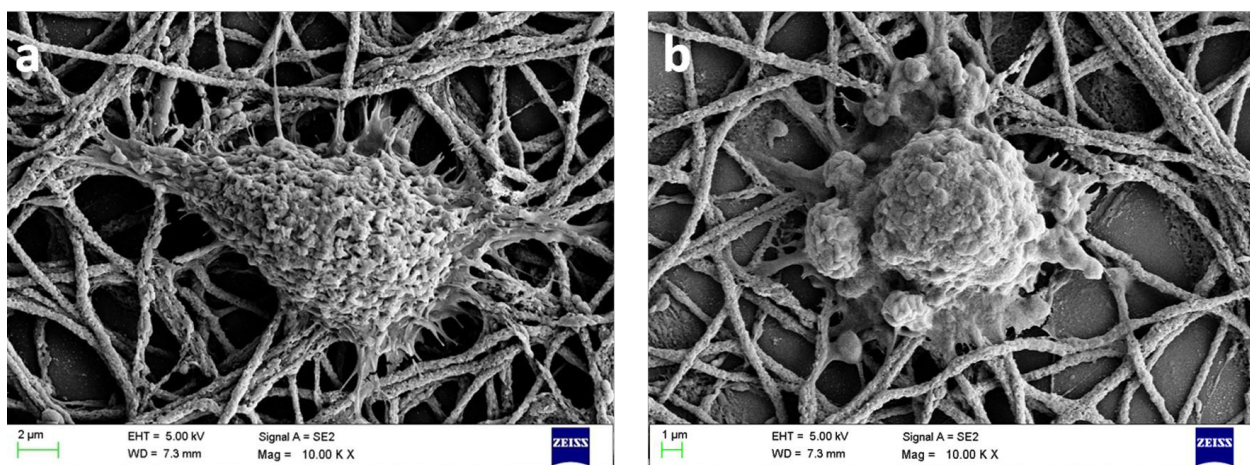


Figure.9 FE-SEM images of A549 and MCF-7 cancer cells seeded over nic@Ag NPS composite nanofiber for period of 24 h, images a and b clearly showing the apoptotic body formation and membrane blebbing in treated cells.

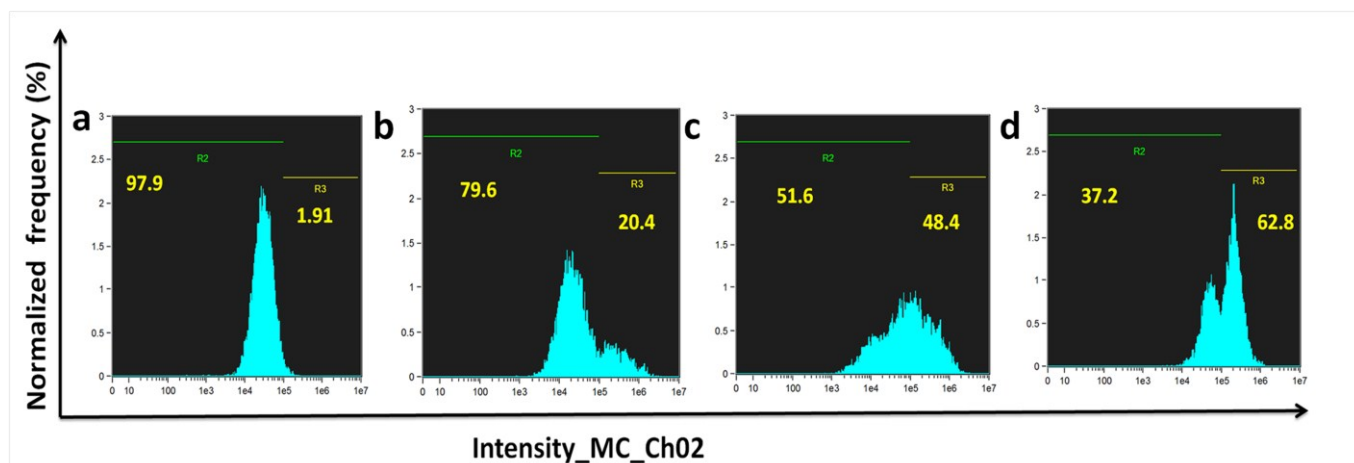


Figure.10 Quantitation of ROS generation by flow cytometric analysis in MCF-7 cells treated with various formulations of nanofibers including control nanofiber, niclosamide, Ag NPs, nic@Ag NPs composite nanofiber shown in image a-d respectively.

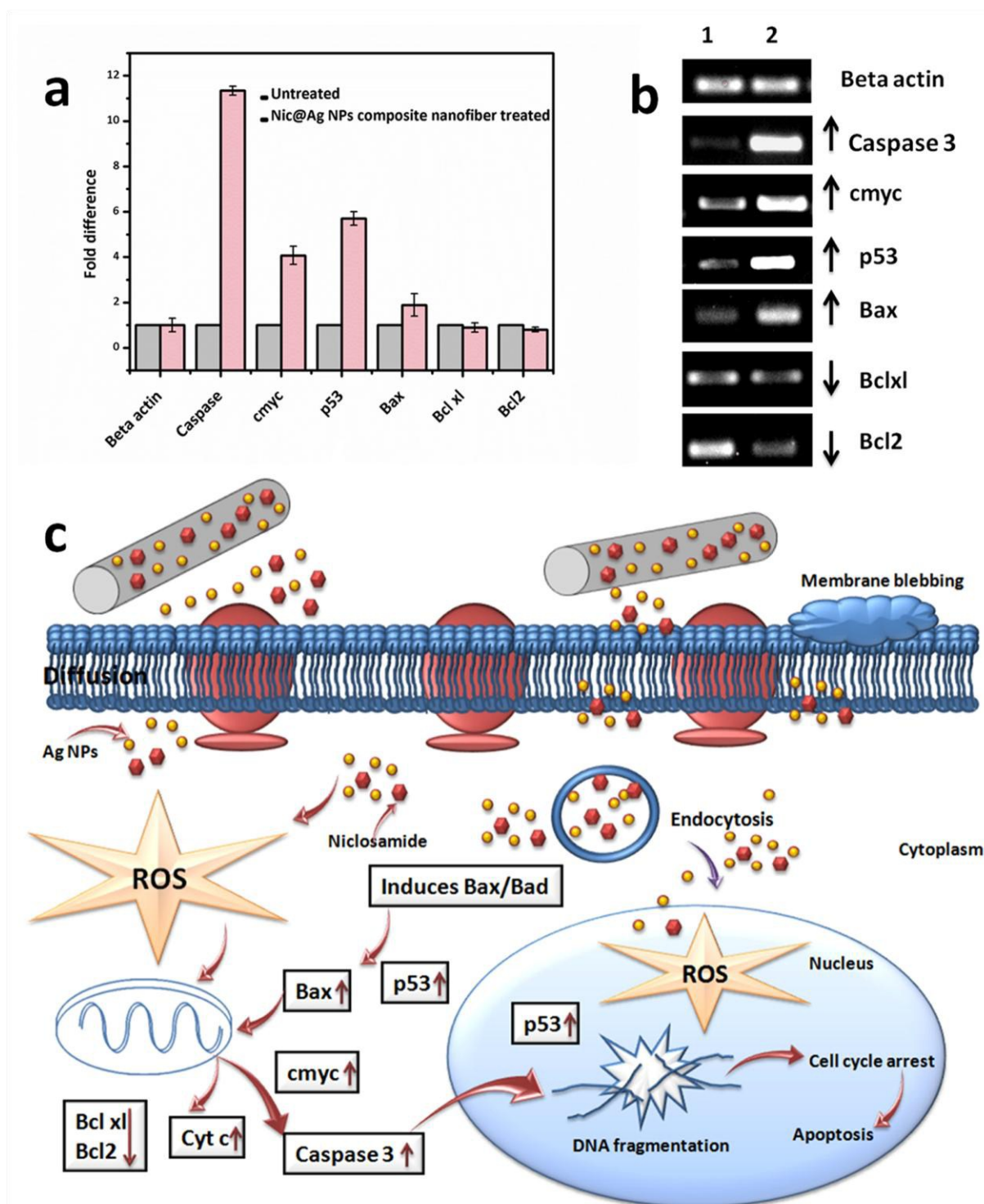


Figure.11 Semi-quantitative RT-PCR analysis of mitochondrial apoptotic signaling pathway induced by nic@Ag NPs composite nanofiber in MCF-7 cells in ROS mediated manner. a) The change in gene expression was expressed as fold difference and done independently thrice. b) Lane 1 and 2 corresponds to control and nic@Ag NPs composite nanofiber treated cells respectively. c) Schematic illustration of probable mechanism of induction of ROS mediated mitochondrial apoptotic cell signaling by nic@Ag NPs composite nanofiber.

Graphical abstract: